ROADWAY SAFETY INSTITUTE

Human-centered solutions to advanced roadway safety

Development and Demonstration of Merge Assist System using Connected Vehicle Technology

Shah Hussain
Zhiyuan Peng
M.I. Hayee

Department of Electrical Engineering
University of Minnesota Duluth

Final Report

REGION 5

CTS 19-06

University of Minnesota Driven to Discover℠ | The University of Akron | Illinois University of Illinois at Urbana-Champaign | Southern Illinois University Edwardsville | Western Michigan University

Technical Report Documentation Page

1. Report No.	2.	3. Recipients Accession No.
CTS 19-06		

4. Title and Subtitle	5. Report Date
Development and Demonstration of Merge Assist System using Connected Vehicle Technology	April 2019
	6.

7. Author(s)	8. Performing Organization Report No.
Shah Hussain, Zhiyuan Peng, and M.I. Hayee	

9. Performing Organization Name and Address	10. Project/Task/Work Unit No.
Electrical Engineering University of Minnesota Duluth 1049 University Drive Duluth, MN 55812	CTS #2015022
	11. Contract (C) or Grant (G) No. DTRT13-G-UTC35

12. Sponsoring Organization Name and Address	13. Type of Report and Period Covered
Roadway Safety Institute Center for Transportation Studies University of Minnesota 200 Transportation and Safety Building 511 Washington Ave. SE Minneapolis, MN 55455	Final Report
	14. Sponsoring Agency Code

15. Supplementary Notes

http://www.roadwaysafety.umn.edu/publications/

16. Abstract (Limit: 250 words)

One potential area to improve driver safety and traffic mobility is around merge points of two roadways, e.g., at a typical freeway entrance ramp. Due to poor visibility because of weather or complex road infrastructure, on many such entrance ramps, it may become difficult for the driver on the merging/entrance ramp to clearly see the vehicles travelling on the main freeway, making it difficult to merge. A fundamental requirement to facilitate many advance driver assistance systems (ADAS) functions including a merge assist system is to accurately acquire vehicle positioning information. Accurate position information can be obtained using either sensor-based systems (camera-based, radar, lidar) or global navigation satellite systems (GPS, DGPS, RTK). For these systems to work well for practical road and weather conditions, advanced techniques and algorithms are needed, which make the system complex and expensive to implement. In this research project, we propose a merge assist system by acquiring the relative positioning of vehicles using standard GPS receivers and dedicated short-range communication (DSRC) based vehicle-to-vehicle (V2V) communication. The DSRC-equipped vehicles travelling on the main freeway and on the entrance-ramp will periodically communicate their positioning information with each other. Using that information, the relative trajectories, relative lane, and position of all DSRC-equipped vehicles travelling on the main freeway will be calculated and recorded in real time in the vehicle travelling on the entrance ramp. Finally, a merge-time cushion will also be calculated, which could potentially be used to assist the driver of the ramp vehicle to safely merge into the freeway.

17. Document Analysis/Descriptors	18. Availability Statement
Dedicated short range communications, Global Positioning System, Vehicle to vehicle communications, Freeways, Ramps (Interchanges)	No restrictions. Document available from: National Technical Information Services, Alexandria, Virginia 22312

19. Security Class (this report)	20. Security Class (this page)	21. No. of Pages	22. Price
Unclassified	Unclassified	51	

Development and Demonstration of Merge Assist System using Connected Vehicle Technology

FINAL REPORT

Prepared by:

Shah Hussain
Zhiyuan Peng
M.I. Hayee
Department of Electrical Engineering
University of Minnesota Duluth

April 2019

Published by:

Roadway Safety Institute
Center for Transportation Studies
University of Minnesota
200 Transportation and Safety Building
511 Washington Ave. SE
Minneapolis, MN 55455

ACKNOWLEDGMENTS

The funding for this project was provided by the United States Department of Transportation's Office of the Assistant Secretary for Research and Technology for the Roadway Safety Institute, the University Transportation Center for USDOT Region 5 under the Moving Ahead for Progress in the 21st Century Act (MAP-21) federal transportation bill passed in 2012.

TABLE OF CONTENTS

LIST OF FIGURES

LIST OF ABBREVIATIONS

- DSRC: Dedicated Short-Range Communication
- GNSS: Global Navigation Satellite Systems
- GPS: Global Positioning System
- DGPS: Differential Global Positioning System
- RTK: Real-Time Kinematic
- V2V: Vehicle to Vehicle
- V2I: Vehicle to Infrastructure
- ADAS: Advance Driver Assistance Systems
- Dr: Relative Distance (Distance between two vehicles w.r.t each other)
- DL: Lateral Distance (Horizontal or lateral distance between two vehicles)
- Ce: Curvature Error (Error introduced in the estimation of Lateral Distance due to the curvature of the road)
- DL': Effective Lateral Distance (Lateral Distance minus Curvature Error)
- θD: Differential Heading (The difference of headings of any two vehicles)
- LW: Lane Width

EXECUTIVE SUMMARY

One potential area to improve driver safety and traffic mobility is around the merge points of the two roadways, e.g., at a typical freeway entrance ramp. To avoid a potential crash, merging vehicles stop or slow down to yield to faster moving traffic before merging and speeding up. Sometimes, drivers of the merging vehicles cannot see the fast-moving vehicles on the main freeway due to natural growth or weather-related effects, e.g., accumulated snow barriers. Occasionally, even when the driver on the merging ramp can see the vehicles travelling on the main road, it is difficult to judge if it is safe to merge. Therefore, a system that could help facilitate the driver of the merging vehicle to safely merge into the freeway would significantly reduce road accidents around the freeway ramp.

The fundamental requirement for many vehicular applications, including a merge assist system and many other intelligent transportation systems (ITSs) and location-based services (LBSs) is to accurately acquire vehicle positioning information. Accurate vehicle positioning information can be obtained using either sensor-based systems (image processing, radar, lidar, etc.) or global navigation satellite systems (GNSSs). Sensor-based systems rely on vision or laser-based sensors to acquire the relative positions of surrounding vehicles. However, environmental factors such as weather, variable lighting conditions, absence of line-of-sight (LoS) or worn-out road markings can adversely affect the performance of these systems. On the other hand, GNSS-based technologies such as global positioning system (GPS) cannot predict the absolute position of a vehicle with lane-level accuracy without using a correction or augmentation system, e.g., differential GPS technology, inertial sensors, gyroscope, and/or high-resolution maps. However, the absolute position of the vehicle has limited interest by itself, particularly for road-safety applications. What is generally needed, is the position relative to the road network and to its various objects of interest such as intersections, road edges, traffic lights, or other vehicles.

In this report, the authors propose a methodology to estimate a merge-time cushion using standard GPS and dedicated short-range communication (DSRC)-based vehicle to vehicle (V2V) communication, which could potentially be used to help the driver of the entering ramp vehicle safely merge into the freeway. Merge-time cushion is the time for the vehicle on the right-most lane of the main freeway to reach the common merging position of the merging vehicle and the vehicle on the right-most lane. This project is divided into three main tasks: acquisition of relative position accuracy, relative lane identification of surrounding vehicles travelling on the main freeway, and finally estimating merge-time cushion.

First, although the absolute position accuracy of today's standard GPS receivers is not sufficient for lane level resolution, relative position accuracy could be potentially sufficient enough. This is due to the fact that a major part of GPS positioning error, caused by atmospheric effects, is highly correlated over a vast geographical area. Therefore, multiple GPS receivers of the same kind on different vehicles in close proximity tend to have a similar atmospheric error at a given time. The common atmospheric error could be canceled out to obtain a more accurate estimate of the relative distance between any two vehicles as compared to the absolute position of each vehicle. Utilizing this approach, we have successfully acquired the relative trajectories of vehicles traveling in multiple lanes toward a merging junction with an accuracy of less than half of the lane width using DSRC-based V2V communication and standard GPS receivers. The

accuracy of the acquired relative trajectory is sufficient to differentiate vehicles traveling in adjacent lanes of a multiple-lane freeway.

Second, relative lane identification serves a critical part in facilitating not only a merge assist system but also many other advance driver assistance systems (ADAS). For example, to safely merge into the freeway, the entering ramp vehicle is required to yield to the traffic travelling on the main freeway, which could potentially interfere with the merging especially the vehicles travelling in the right-most lane of the freeway. Therefore, it is crucial that we know the relative lane and position of all the vehicles on the freeway travelling toward the merging junction. The relative lane of surrounding vehicles is estimated using lateral distance between two vehicles. Lateral distance can be precisely estimated using Point-Line equation if the vehicles are travelling on a straight road segment. However, this estimation of lateral distance using the Point-Line equation becomes erroneous for a curved road segment because of the error due to the degree of curvature of the road. Hence, lateral distance calculated using the Point-Line equation can no longer be used as such for relative lane identification. The increase in lateral distance depends on the curvature of the road and can be estimated using differential heading and relative distance between two vehicles. For simplicity, the increase in lateral distance between the two vehicles is termed a curvature error in this report. We have worked on normalizing this curvature error to find an effective lateral distance that can be used for accurate relative lane identification for both straight and curved road segments simultaneously. We performed extensive field tests on I-13, a two-lane freeway in Duluth, Minnesota, and the results showed that the relative lane and position of surrounding vehicles can be identified in real time with 100% accuracy regardless of the degree of curvature of the road when the distance between the two vehicles is less than 50 m.

Finally, merge-time cushion is calculated, which is defined as the time required for the vehicle in the right-most lane of the freeway to arrive at the common merging point that could potentially interfere with the merging of the entering ramp vehicle. DSRC-equipped vehicles travelling on the freeway and on the merging-ramp will periodically communicate important traffic parameters such as their location, direction of travel, and speed, to each other. Using that information, the relative trajectories of all DSRC equipped vehicles travelling on the freeway will be acquired and then processed in real time to identify their relative lane and position. Once the relative lane and position of the vehicles traveling on the freeway are identified, a merge-time cushion will be estimated, which could potentially be used as an important parameter to develop a merge assist application. Two distinct merging scenarios and their solution are presented based on the geometry of the road. However, more tests need to be conducted to test the performance of the proposed methodology for merge-time estimation.

CHAPTER 1: INTRODUCTION

1.1 BACKGROUND

Intelligent Transportation Systems joint program office of the US Department of Transportation continues to be committed to the use of dedicated short-range communication (DSRC) for active safety applications using vehicle to vehicle (V2V) and/or vehicle to infrastructure (V2I) communication [1]. One potential area to improve driver safety and traffic mobility is around merge points of the two roadways, e.g., at a typical freeway entrance ramp. Usually, the speed of the vehicles travelling on a freeway is much higher than the speed of the vehicles on a merging ramp. To avoid a potential crash, merging vehicles stop or slow down to yield to faster moving traffic before merging and speeding up. Sometimes, drivers of the merging vehicles cannot see the fast-moving vehicles on the main freeway due to natural growth or weather-related effects, e.g., accumulated snow barriers. Occasionally, even when the driver on the merging ramp can see the vehicles travelling on the main road, it is difficult to judge if it is safe to merge. While a cautious driver could disturb the traffic flow by waiting long enough, a rushed driver could jeopardize safety. According to one study, 36% of the total freeway accidents analyzed were on the entrance ramps [2], and according to another study, nationally 20–30% of total truck accidents occur on or near ramps [3].

When vehicles are merging into a freeway, both driver safety and traffic efficiency could be at risk if not managed properly. During the rush hour, ramp metering is used to improve traffic efficiency on freeways, which also indirectly improves driver safety by reducing the risk of crashes [4]. In research to provide merge assistance using DSRC-based V2I and V2V communication, three application scenarios, namely emergency vehicle routing, merge assistance, and pedestrian crossing warning, were chosen as desired goals, and a merge assistance scenario for increasing safety and mobility on motorway ramps was depicted focusing on the merging of heavy vehicles, but the work was limited to the conceptual level [5]. Similarly, some theoretical work has also been done on collision avoidance and cooperative adaptive cruise control systems using DSRC-based V2V communication [6 - 10]. However, no practical system has been demonstrated, to our knowledge, using DSRC-based V2I and/or V2V communication to facilitate safe merging. Critical safety applications, such as merge assist or lane change assist systems, require only the relative positions of surrounding vehicles with lane level resolution to allow a given vehicle to differentiate the vehicles in its own lane from the vehicles in adjacent lanes [11]. Therefore, in the approach presented in this research, we have focused on acquiring the relative trajectories of surrounding vehicles using standard global positioning system (GPS) receivers—without any additional correction system—and DSRC-based V2V communication. Our approach to acquire relative trajectories is based on the fact that a major part of GPS positioning error, caused by atmospheric effects, is highly correlated over a vast geographical area [12] [13]. Therefore, multiple GPS receivers of the same kind on different vehicles in close proximity tend to have a similar atmospheric error at a given time. The common atmospheric error could be canceled out to obtain a more accurate estimate of the relative distance between any two vehicles as compared to the absolute position of each vehicle. Utilizing this approach, we have successfully acquired relative trajectories of vehicles traveling in multiple lanes, as well as identified the relative lane of vehicles travelling toward a merging junction using DSRC-based V2V communication and standard GPS

receivers. The accuracy of the relative lane identification is sufficient to facilitate many critical advance driver assistance system (ADAS) functions such as a merge assist system, etc.

1.2 PROJECT OVERVIEW

The conceptual approach of the project is described in Figure 1.1, where traffic is shown to merge into a fast-moving, two-lane freeway. Each vehicle approaching the merging junction is assumed to be equipped with a DSRC device and a GPS receiver. All vehicles on the main freeway periodically communicate their position information (latitude and longitude) to the merging vehicle (shown in yellow) using DSRC-based V2V communication. After the DSRC device of the merging vehicle acquires the position information of all the vehicles around the merge junction, it calculates necessary parameters to estimate a merge-time cushion, which helps the driver to safely merge into the freeway. These necessary parameters are: acquiring the accurate relative trajectories of the vehicles; identifying the relative lane and position of the vehicles around the merging junction; and identifying the vehicle of concern that could interfere with the merging of the ramp vehicle.

1.3 OBJECTIVES

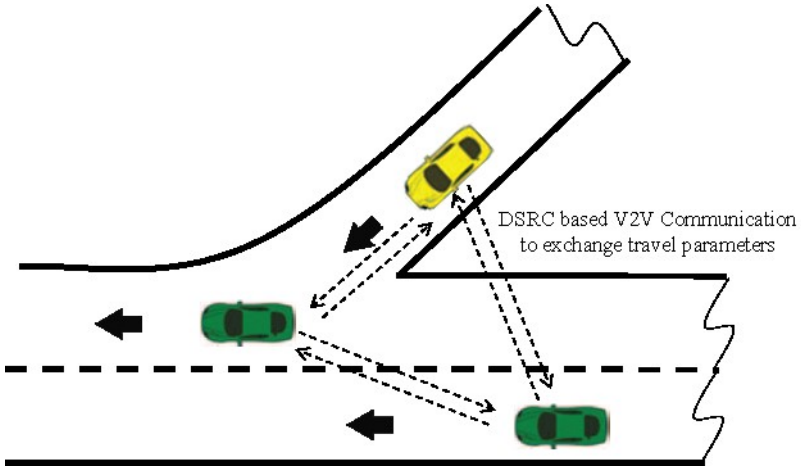

Figure 1.1 The schematic diagram of a vehicle travelling toward a two-lane freeway merge junction. All vehicles' trajectories will be recorded and processed in real time in the vehicle trying to merge the freeway (shown in yellow).

The goal of this project is to design and implement a merge assist system using DSRC-based V2V communication, which helps the driver of the ramp vehicle to safely merge into the freeway. The main objectives to achieve this task are:

1.3.1 Acquisition of Relative Position Accuracy

One of the critical aspects in the successful accomplishment of the proposed project is to accurately estimate travel parameters, e.g., location, speed, and direction of travel. Although the absolute position accuracy of today's standard GPS receivers is not very accurate, relative position accuracy is much more

reliable. This is due to the fact that a major part of GPS positioning error, caused by atmospheric effects, is highly correlated over a vast geographical area [12, 13]. Therefore, multiple GPS receivers of the same kind on different vehicles in close proximity tend to have a similar atmospheric error at a given time. The common atmospheric error could be canceled out to obtain a more accurate estimate of the relative distance between any two vehicles as compared to the absolute position of each vehicle. Utilizing this approach, we have successfully acquired the relative trajectories of vehicles traveling in multiple lanes toward a merging junction with an accuracy of less than half of the lane width using DSRC-based V2V communication and standard GPS receivers [14]. The accuracy of the acquired relative trajectory was sufficient to differentiate vehicles traveling in adjacent lanes of a multiple-lane freeway.

1.3.2 Relative Lane and Position Identification of Surrounding Vehicles

To safely merge into the freeway, the ramp vehicle is required to yield to the traffic travelling on the main freeway, which could potentially interfere with merging, especially vehicles travelling in the right-most lane of the freeway. Therefore, it is crucial that we know the relative lane and position of all the vehicles on the freeway travelling toward the merging junction.

The relative lane of any two vehicles on a straight road segment is decided based on the lateral distance (D_L) between the two vehicles, as shown in Figure 1.2(a). If the absolute value of D_L ($|D_L|$) is less than ½ of the lane width (LW) of the road, the two vehicles are said to be in the same lane. Similarly, if $|D_L|$ is more than ½ LW but less than 1½ LW, the two vehicles are said to be in the adjacent lanes. The sign of D_L helps distinguish the right lane from the left lane. Figure 1.2(a) illustrates that D_L can be precisely estimated using a Point-Line equation because of the road being a straight segment. However, this estimation of D_L using the Point-Line equation becomes erroneous for a curved road segment because of the error caused by the degree of curvature of the road, as illustrated in Figure 1.2(b). Although on a curved road segment (Figure 1.2b) the true D_L between the two vehicles should be less than ½ LW because they occupy the same lane, the calculated D_L between the two vehicles appears to be larger than LW. Hence, D_L calculated using the Point-Line equation can no longer be used as such for relative lane identification. Therefore, it is necessary to first estimate the increase in D_L to adjust the calculated D_L between the two vehicles before estimating their relative lane. The increase in D_L depends on the curvature of the road and can be estimated using differential heading (θ_D) and relative distance (D_r) between the two vehicles. For simplicity, the increase in D_L between the two vehicles is termed a curvature error (C_e) in this report.

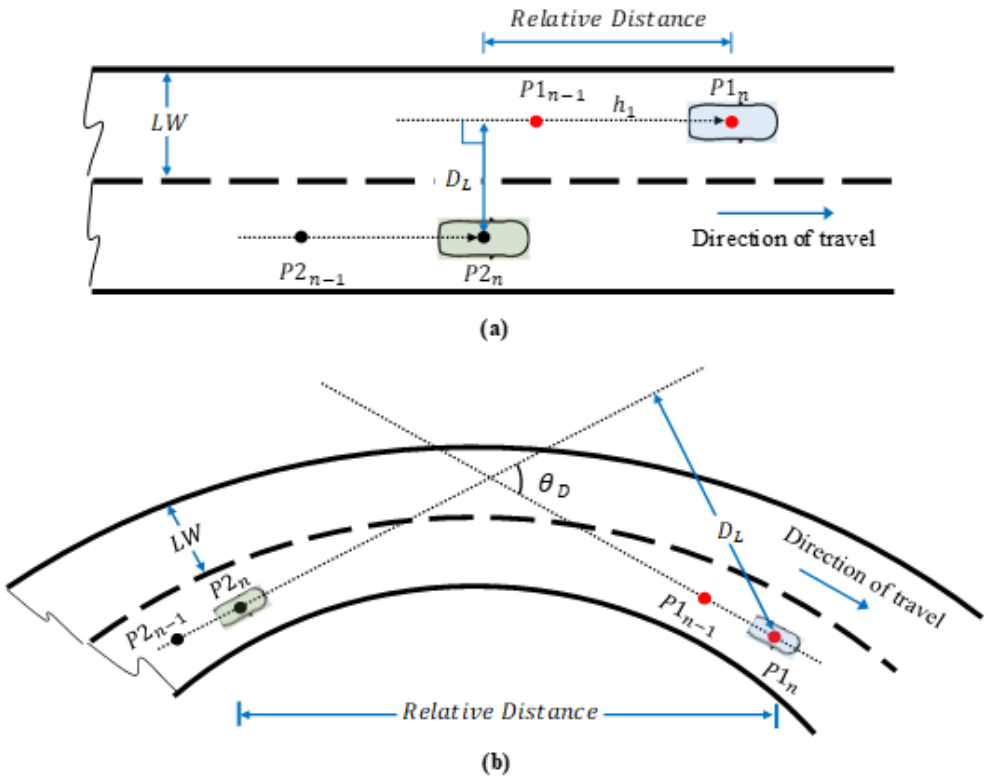

Figure 1.2 Schematic diagram of two vehicles illustrating the concept of relative lane identification on (a) straight road and (b) curved road. Where $P1n$ and $P2n$ are the position coordinate points of vehicle 1 and vehicle 2 at $t = n$, and $P1n–1$ and $P2n–1$ are the position coordinate points of vehicle 1 and vehicle 2 at $t = n–1$. LW is the lane width of the road.

We have worked on normalizing this curvature error to find an effective lateral distance that can be used for accurate relative lane identification for both straight and curved road segments simultaneously. We performed extensive field tests on I-13, a two-lane freeway in Duluth, Minnesota, and the results showed that the relative lane and position of surrounding vehicles can be identified in real time with 100% accuracy regardless of the degree of curvature of the road when the distance between the two vehicles was less than 50 m.

1.3.3 Merge-Time Cushion

Merge-time cushion is the time for the vehicle on the right-most lane to reach the common merging position, M, of the merging vehicle and the vehicle on the right-most lane as shown in Figure 1.3. Once the DSRC communication is established between the vehicles on the main freeway and the vehicle on the merge junction, and relative positions of the vehicles are calculated in the DSRC device of the vehicle on the merge junction, it will be determined which vehicle is on the right-most lane of the freeway that could interfere with the merging of the vehicle on the merge junction. Once lane determination is confirmed, using the speed of the vehicle on the right-most lane, a merge-time cushion will be estimated to show

how much time is needed for the right-most vehicle to reach the common merging point 'M'. The merge-time cushion will be updated continuously in real time and could change slightly depending on the speed of the vehicle on the right-most lane of the freeway and/or the geometry of the merging ramp. Please note that if there is only one vehicle traveling toward the merging junction on the freeway, it will be considered to be in the right-most lane. Furthermore, the leading vehicle in the right-most lane toward the merging junction will be chosen for merge time cushion calculation.

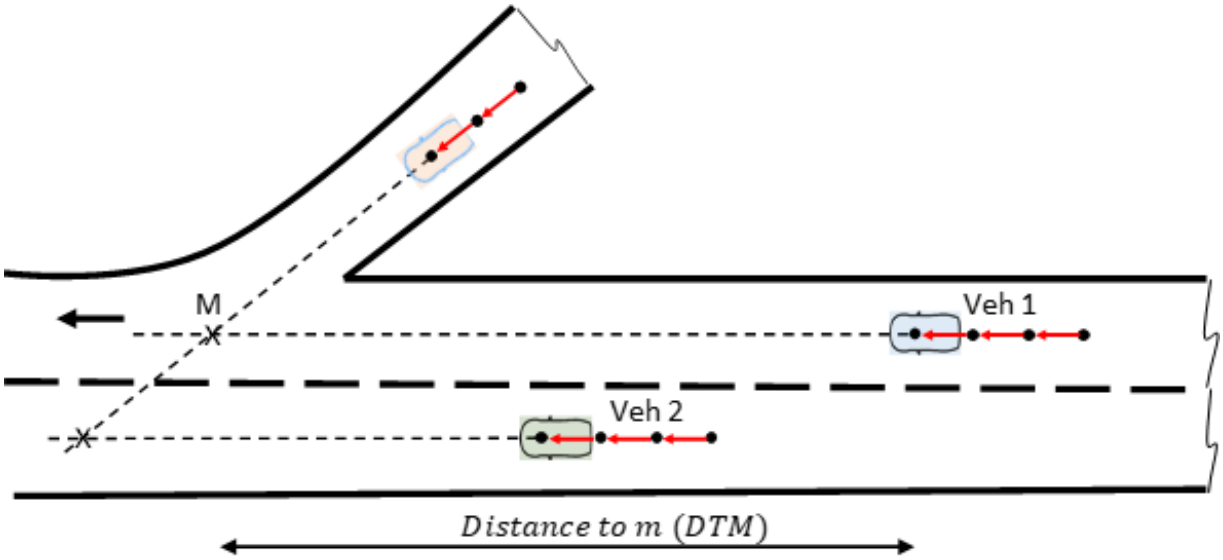

Figure 1.3 Typical merging scenario, where vehicle 1 is travelling toward the common merging point 'M' and could interfere with the merging of the ramp vehicle.

1.4 RELATED WORK

Autonomous, or self-driving cars, require a high level of situational awareness to operate safely and efficiently in real-world conditions [15]. For fully autonomous vehicles and ADAS such as lane keeping, blind spot detection, merge assist system, vehicle detection, or auto cruise control, it is necessary to know the position of the car in the lane it occupies [16-18]. However, the absolute position of the vehicle has limited interest by itself, particularly for road safety applications. What is generally needed, is the vehicle's position relative to the road network and to its various objects of interest such as intersections, road edges, traffic lights, or other vehicles [16].

Position information is a fundamental requirement for many vehicular applications such as navigation, intelligent transportation systems (ITSs), and location-based services (LBSs) [19]. Accurate positioning information can be obtained using either sensor-based systems (image processing, radar, lidar etc.) or global navigation satellite systems (GNSSs) [14]. Sensor-based systems rely on vision or laser-based sensors to acquire the relative positions of surrounding vehicles [20-23]. However, environmental factors such as weather, variable lighting conditions, absence of line-of-sight (LoS), and worn-out road markings can adversely affect the performance of these systems [24]. Guizhen Yu et al. in [25] proposes a real-time lane detection method using image processing, which despite being complex and relatively expensive,

does not work well when an obstacle on the road is similar to lane lines, or where the lane line is missing for a long time. Most of these vision or sensor-based systems such as proposed in [26] and [27] suffer in challenging environments. On the other hand, GNSS-based technologies such as GPS cannot predict the position of a vehicle with lane-level accuracy without using a correction or augmentation system, e.g., differential GPS technology, inertial sensors, gyroscope, and/or high-resolution maps [28-32]. There are some reports of achieving lane-level accuracy using differential GPS receivers and/or image processing techniques, which makes the system complex and relatively expensive [33-35]. Therefore, a system that can efficiently acquire the relative trajectories of the vehicle using inexpensive equipment would be an important milestone to facilitate not only a merge assist system but also many other basic safety applications.

1.5 DEDICATED SHORT-RANGE COMMUNICATION (DSRC)

DSRC is a bi-directional short-to medium-range wireless communication technology designed for automotive communication. A conceptual demonstration of this technology is shown in Figure 2.1. DSRC applications primarily targets the transportation industry and the following features of DSRC technology enable it to improve drivers' safety and traffic mobility.

• Designated licensed bandwidth: Federal Communications Commission (FCC) exclusively allocated 75 MHz bandwidth in the 5.9 GHz band.

• Full protocol support: IEEE 802.11p extends 802.11 wireless communication protocol family to support critical safety applications.

• Fast network acquisition: Active safety applications require the immediate establishment of communication and frequent updates.

• Low latency: Active safety applications must recognize each other and transmit messages to each other in milliseconds without delay.

• High reliability when required. DSRC works in high vehicle speed mobility conditions and delivers performance immune to extreme weather conditions (e.g., rain, fog, snow, etc.).

The application of DSRC technology falls into two categories: V2V communications and V2I communications.

1.5.1 Vehicle to Vehicle (V2V) communications

DSRC technology enables vehicles to exchange their travel information on the road. For example, a vehicle's travel speed and travel direction can be shared with other vehicles, so that potential collisions could be prevented. Drivers' awareness of surrounding vehicles also can be improved. This is especially helpful when drivers are near merging ramps or intersections where there is limited or no line-of-sight to the other vehicles. Augmenting vehicular platoon with DSRC technology can help it achieve better speed and distance control.

1.5.2 Vehicle to Infrastructure (V2I) communications

V2I communications further explore the potentials of DSRC technology. For example, DSRC communication devices installed on frequently congested road intersections can help broadcast messages to nearby vehicles to inform drivers of choosing alternative routes. Near a slippery road section or sharp turn area, well-placed DSRC devices could give warnings to drivers about incoming high-risk road conditions.

CHAPTER 2: ACQUISITION OF RELATIVE TRAJECTORIES OF SURROUNDING VEHICLES USING GPS AND DSRC BASED V2V COMMUNICATION

Critical safety applications such as merge-assist or lane-change-assist systems require only the relative positions of surrounding vehicles with lane-level resolution to allow a given vehicle to differentiate the vehicles in its own lane from the vehicles in adjacent lanes [11]. Therefore, in the approach presented in this report, we have focused on acquiring the relative trajectories of surrounding vehicles using standard GPS receivers—without any additional correction system—and DSRC-based V2V communication. Our approach to acquire relative trajectories is based on the fact that a major part of GPS positioning error, caused by atmospheric effects, is highly correlated over a vast geographical area [12] [13]. Therefore, multiple GPS receivers of the same kind on different vehicles in close proximity tend to have a similar atmospheric error at a given time. The common atmospheric error could be canceled out to obtain a more accurate estimate of the relative distance between any two vehicles as compared to the absolute position of each vehicle. Utilizing this approach, we have successfully acquired relative trajectories of vehicles traveling in multiple lanes toward a merging junction with lane level accuracy using DSRC-based V2V communication and standard GPS receivers.

2.1 WHAT IS DGPS?

DGPS stands for Differential GPS. It is an augmented GPS system, which have better accuracy (<10 cm) than the traditional GPS system. The relative accuracy concept in this project originated from the methodology being used in DGPS system. Traditionally, GPS receivers receive signals from navigation satellites and then using triangulating method to determine its own position. What makes DGPS system different from the classic GPS system is its ground reference station, which is capable of broadcasting another position correction message to GPS receivers.

Reference Station is a known position GPS receiver constantly receiving navigation satellite signals. It calculates its measured position and finds the difference between measured position and its real location. Then this difference is broadcasted as correction message to nearby GPS receivers. As the other GPS receivers receive both the GPS signals and the correction message, it subtracts the difference reported by reference station from its calculated position, which gives a better position estimation. This process is illustrated in Figure 2.1. The key of this correction mechanism is based on the fact that achievable accuracy degrades at an approximate rate of 1 m for each 150km distance from the broadcast site. So as the distance between a GPS receiver and reference station is within a reasonable range, the accuracy of DGPS system is better than what standalone GPS system can deliver.

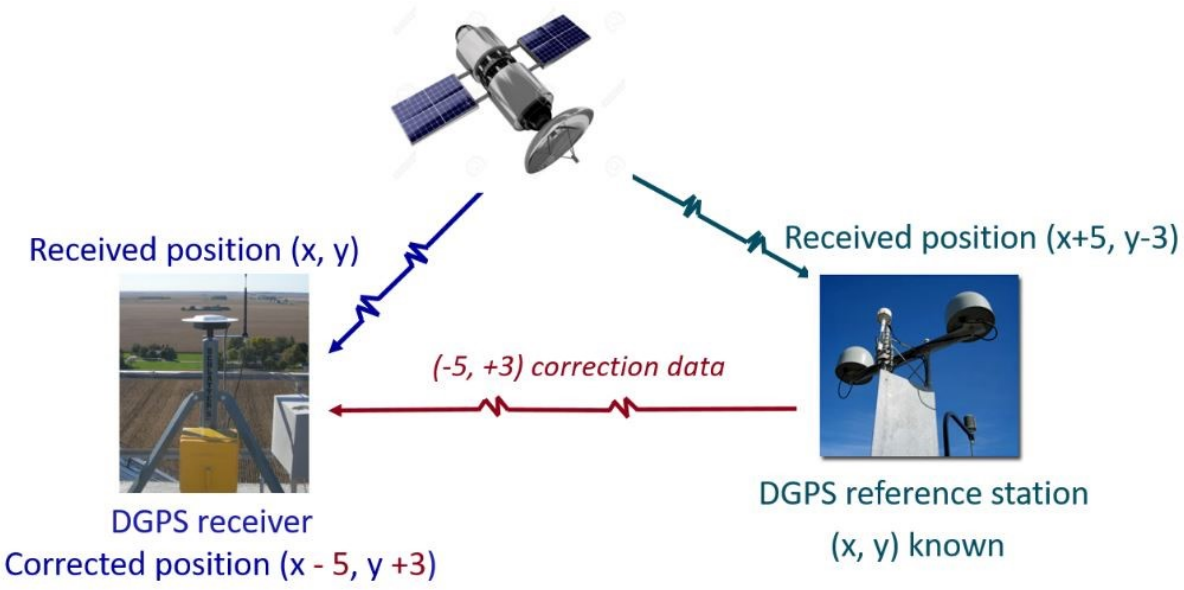

Figure 2.1: DGPS Principle

2.2 GPS ERROR MODELLING

Our approach utilizes standard GPS receivers and DSRC-based V2V communication to acquire the relative of surrounding vehicles. The absolute position accuracy of a standard GPS receiver is in the range of 3–5m [36]. This means that a GPS receiver can estimate the position of a vehicle within a circle with a radius of 3–5m, as shown in Figure 2.2, where the true position of the vehicle at a given time is shown by a green dot and the red dot shows the estimated position by the GPS receiver. The error vector from the true position to the estimated position represents the GPS position error. The total GPS position error is a combination of multiple errors resulting from different sources. Generally, the combined GPS position error is a result of three major errors: mechanical error, satellite ephemeris error, and atmospheric error.

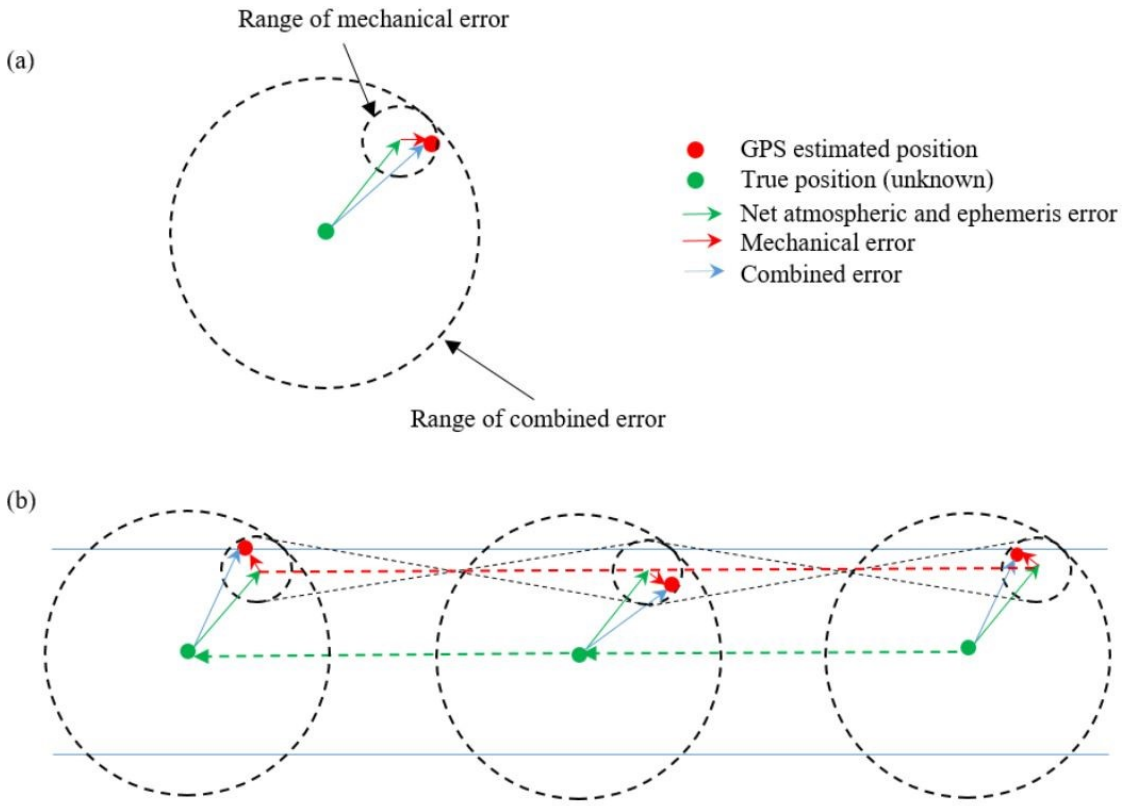

Figure 2.2 Conceptual GPS receiver error model of a single GPS receiver showing ranges of different GPS error types for (a) a stationary vehicle at a single time instance and (b) a moving vehicle at three adjacent time instances.

2.2.1 Static Error Analysis

The mechanical GPS error is caused by inherent noise or clock jitter of the crystal oscillator used in the GPS receiver, thermal effects, manufacturing differences, and residual mathematical error due to quantization and rounding [37-38]. Satellite ephemeris error is due to the fact that the expected orbital positions of the GPS satellites that the GPS receiver needs to estimate its own position, could be different than actual satellite positions.

2.2.1.1 Atmospheric Errors

Atmospheric error, the most significant portion of the combined GPS error, is caused by atmospheric effects that cause the GPS signal to bend while it travels through the atmosphere. Of all three errors, mechanical error is the only one that can vary randomly from one GPS receiver to another at any given time. It can also vary in the same GPS receiver with each subsequent position estimate over time. On the other hand, both ephemeris and atmospheric errors do not vary significantly for multiple GPS receivers in close geographical and temporal proximity. This is because atmospheric disturbances will remain the same over a wide geographical area and do not rapidly change with time [12-13].

2.2.1.2 Ephemeris Error

Similarly, ephemeris error will remain almost the same for the satellite constellation used by GPS receivers in close proximity to each other [39]. Theoretically, a GPS-estimated position can be anywhere in the larger circle as shown in Figure 2.2(a), representing the range of combined GPS error. However, after a GPS receiver gets locked to certain satellites to estimate its position, its subsequent position estimates will not randomly vary over the entire large circle because atmospheric and ephemeris errors will remain the same for a considerable period of time.

2.2.1.3 Mechanical Error

On the other hand, mechanical error can randomly vary in every new position estimate in any GPS receiver. The size of mechanical error is comparatively much smaller than the other two errors, which is highlighted by the relative sizes of the two circles in Figure 2.2(a). Therefore, subsequent estimates of the same position by a given GPS receiver will remain confined to a smaller circle shown in the Figure 2.2(a), representing the range of mechanical error.

2.2.1.4 Multipath Error

In addition to the three errors described above, multipath error can significantly degrade the position estimation accuracy for any GPS receiver. Multipath error occurs when GPS signals arrive at the receiver antenna through multiple paths as a result of reflections from surrounding objects (e.g., high-rise buildings or overhead bridges) [40]. Multipath error is significant in urban areas where a roadway is surrounded by high-rise buildings. However, in rural and suburban areas, multipath error can be negligibly small and the significant errors are mechanical, ephemeris, and atmospheric, as described above.

2.2.2 Dynamic Error Analysis

Figure 2.2(a) illustrated GPS receiver errors in static conditions. When such a GPS receiver is placed in a moving vehicle, it can be used to acquire a vehicle's trajectory by periodically estimating its position. This concept is illustrated in Figure 2.2(b), where three adjacent GPS positions of a fast-moving vehicle on a freeway (with minimal multipath error) are shown as red dots. Each adjacent estimated position will vary only within the small circle (the mechanical error range) as opposed to randomly changing over the larger circle because the atmospheric and ephemeris errors will remain the same for each estimate. Consequently, the trajectory obtained by the GPS receiver may vary randomly, but the maximum variations will be limited to the zigzag pattern shown in Figure 2.2(b). The mean trajectory obtained by the GPS receiver (shown by the red dashed line) will have an offset from the true trajectory (shown by the green dashed line), but it will be a fixed offset and its size will be determined by the magnitude of net atmospheric and ephemeris error. Furthermore, the variance of the trajectory obtained by the GPS receiver will be determined by the magnitude of the mechanical error of the GPS receiver, which is generally small in size.

2.3 THEORY VALIDATION

To validate our relative accuracy theory, we planned to acquire real-time relative trajectories of the vehicles travelling on two separate roads towards a merging junction, using DSRC based V2V communication. The conceptual approach of the proposed system is described in the left side of Figure 2.3, where traffic is shown to merge on a fast-moving single-lane road. Each vehicle approaching the merging junction is assumed to be equipped with global positioning system (GPS) receiver and DSRC equipment. Using the GPS technology and DSRC based V2V communication, critical travel parameters e.g., vehicle location, speed, and direction of travel will be periodically acquired and communicated to the surrounding vehicles. All this information will be processed in each vehicle present either on the fast-moving road or on the merging road.

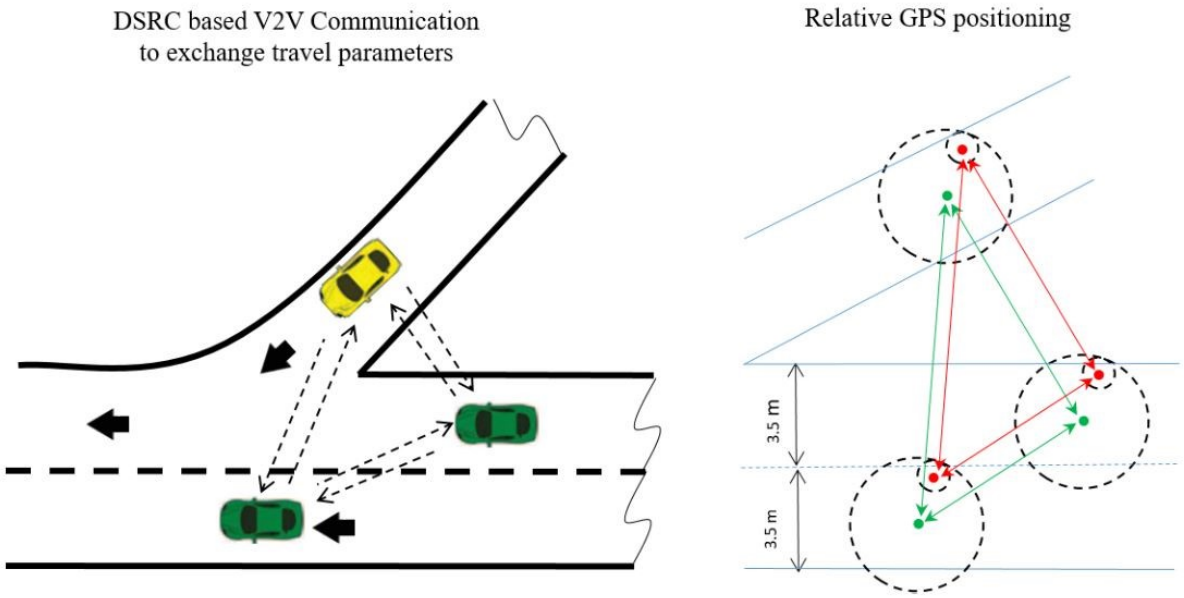

Figure 2.3 The conceptual approach of the proposed system. Left side: DSRC based V2V communication. Right side: Relative GPS positioning

After applying the DGPS principle and following the GPS error model, we will be able to measure the relative distance between the two vehicles. This idea is conceptually shown on the right side of Figure 2.3, where the positions estimates obtained by two ordinary GPS receivers of the two vehicles on two different roads (one on the main road and one on the merging road) are shown as red dots. Please note that the green dots are actual positions of the vehicles and the red dots are estimated locations by ordinary GPS receivers. The error in the absolute position (bigger circle around actual position) of each of these vehicles is larger than the lane width (3.6 m) but the error in the relative distance between the two vehicles will be much less (smaller circle).

2.3.1 DSRC Communication and Data Logging

We have developed the software for transmitting and receiving the travel parameters between multiple DSRC onboard units (OBUs) using wireless access in vehicular environments (WAVE) protocols. The travel information is encapsulated in Basic Safety Message based on SAE J2735 standard. We first achieved this by using older model Savari DSRC devices, S100, and achieved the same functionality using newer model of Savari Devices, S103 as well as using Arada LocoMate 200 devices Figure 2.4. Since each vehicle will be simultaneously transmitting to, and receiving from its surrounding vehicles using DSRC devices, we need to implement our software in a way that it supports bi-directional communications as well as data logging in each reception and transmission interval.

Figure 2.4 DSRC onboard units: Savari S103 and Arada Locomate 200

2.3.2 Preliminary Tests

In order to validate our relative accuracy theory, we performed our initial tests on Arrowhead Road in Duluth, MN. As shown in Figure 2.5, we placed three Savari GPS receivers on the roof our test vehicle in a straight line with equal spacing between them. We recorded the vehicle's trajectory using these three GPS receivers while it was driving within a straight lane. The GPS receivers and their corresponding trajectories are color coded in following figures. In this test, we were trying to qualitatively evaluate the relative GPS accuracy of multiple GPS receivers within close proximity. We expected that the trajectories of these three GPS receivers stay close to each other. The result of this test is shown in Figure 2.6. The vehicle is driving from the right of the figure to the left. GPS points of 100-meter data are plotted on the Google map. As we expected, the trajectories of these GPS stay very close to each other. They were almost overlapping with each other, although a closer look of the data revealed that these three trajectories were not perfectly staying on the same line and the 2nd GPS receiver appeared to stay closer to the 3rd GPS receiver than it actually did.

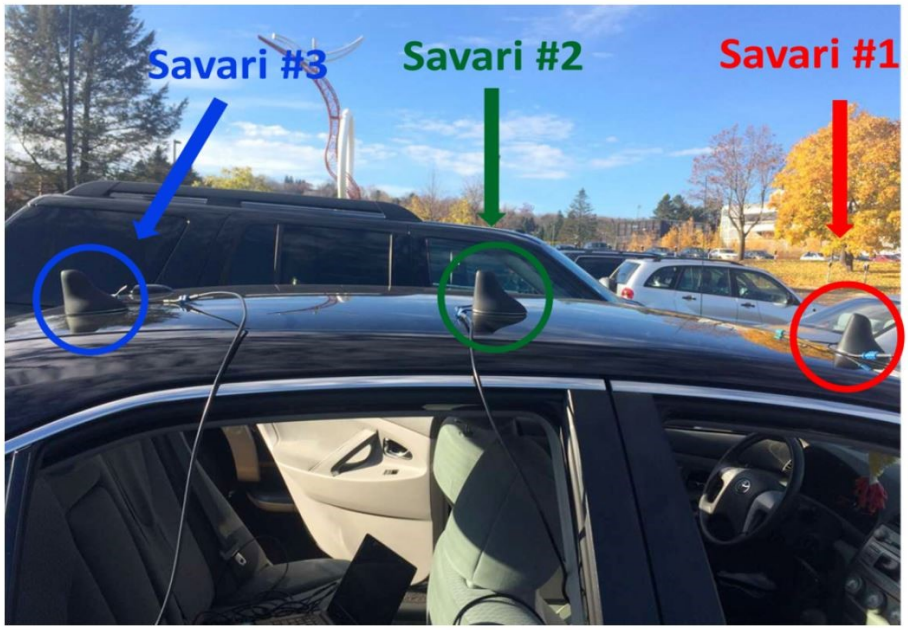

Figure 2.5 Preliminary test setup: Three Savari S103 GPS receivers placed on the top of the vehicle with equal spacing.

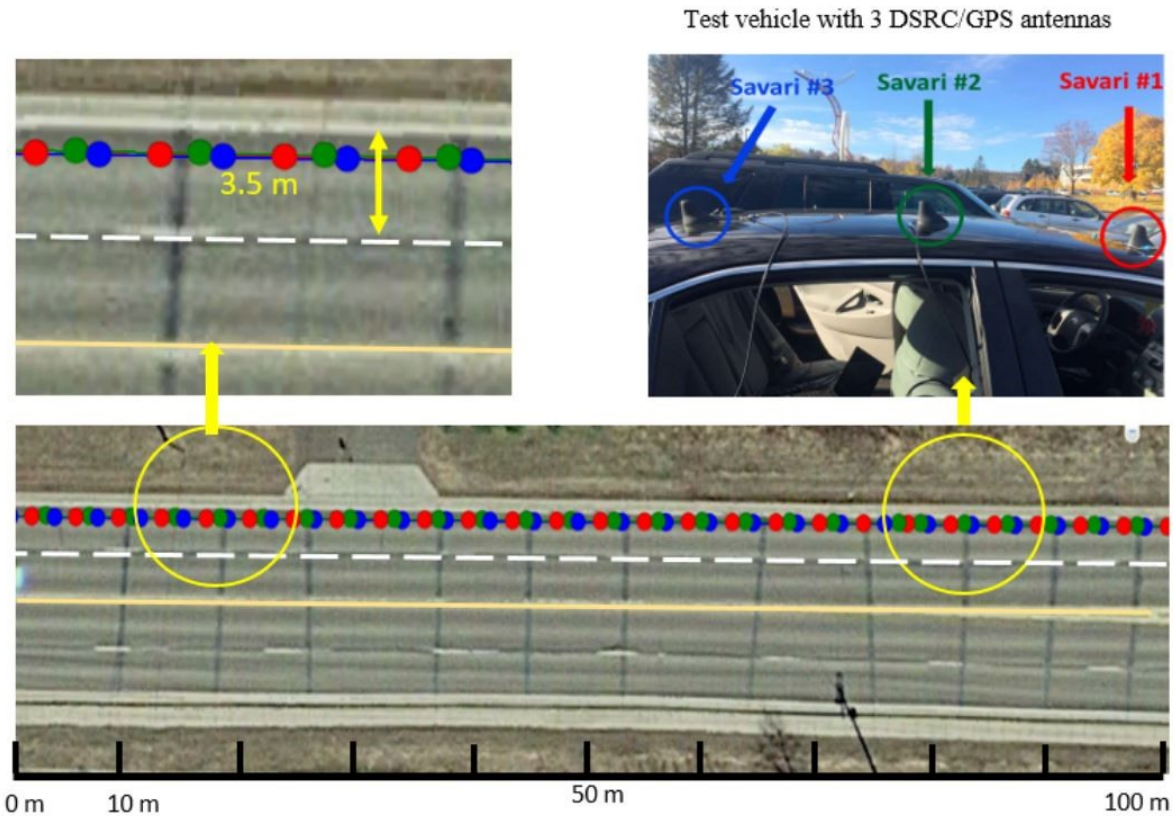

Figure 2.6 Preliminary test results: The top left figure shows a zoomed-in view of the recorded trajectories. The lane width is 3.5 meters as indicated in the figure.

This promising result confirmed two points for us:

1) The trajectories received by GPS is not zig-zagged as shown in Figure 2.7b. Instead, the error of one particular GPS receiver was very stable and we believe this is the reason why the trajectory of each GPS receiver appeared to be a straight line as shown in Figure 2.7a.

2) The relative accuracy of these three GPS receivers is noticeably less than the lane width. As shown in left top figure in Figure 2.6.

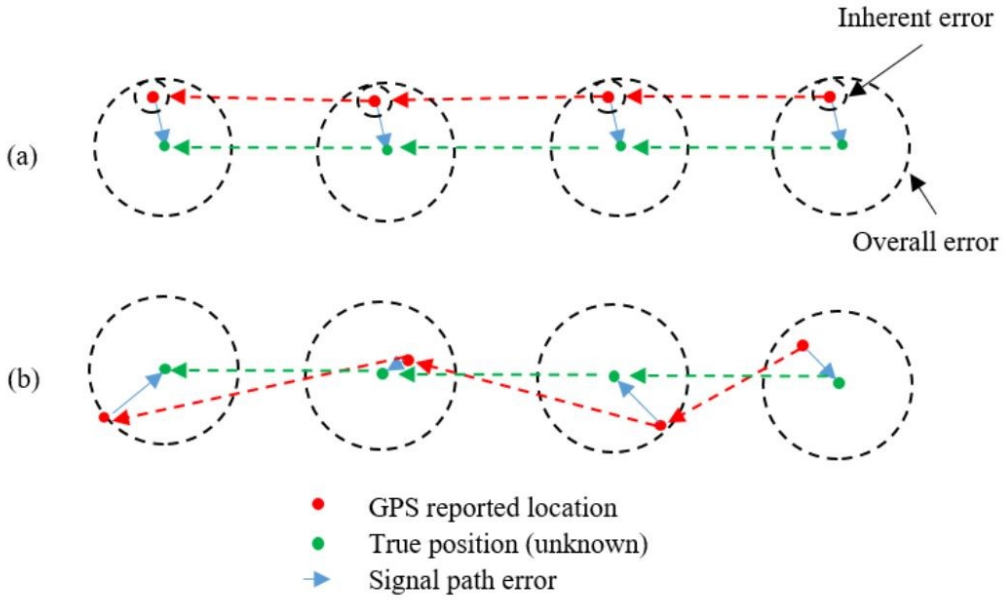

Figure 2.7 Preliminary test results: The top left figure shows a zoomed-in view of the recorded trajectories. The lane width is 3.5 meters as indicated in the figure.

2.3.3 Regular Street Tests

In the regular street field trials, we used two vehicles equipped with DSRC devices and GPS receivers travelled on a two-lane road (W Arrowhead Rd). The speed limit on this road was 45 MPH. We collected data with two scenarios: (i) lane switching scenario, and (ii) lane merging scenario.

2.3.3.1 Lane Switching Scenario

This field trial was conducted on W Arrowhead Rd with two vehicles having DSRC devices traveling in the same direction on two adjacent lanes. The total travelled distance was a little over one kilometer. The two vehicles started on two adjacent lanes and switched lanes in the middle of the trial. We acquired the trajectories of the two vehicles via DSRC devices which recorded GPS position of each vehicle at 5 Hz. We repeated this test twice, first using Arada LocoMate 200 on both vehicles and then using Savari S100 on both vehicles. Please note that we did not have Savari S103 devices at the time of the field tests. After acquiring the GPS trajectories in long-lat format, we converted the trajectories to X-Y format based on the Universal Transverse Mercator (UTM) system. A portion of acquired trajectories of the two vehicles in X-

Y format are shown in Figure 2.8 using Arada Locomate200 devices. The blue and red dotted lines show the relative positions of the two vehicles with respect to each other. The time line shows the relative position of the two vehicles at any given time. Please note that vehicle on the right lane (represented by red dotted line) was a little ahead of the vehicle on the left lane. For reference, we have also shown the relative position of the lane boundaries of the two lanes on which the two vehicles were driven. We used position coordinates from Google Earth to show the lane boundaries.

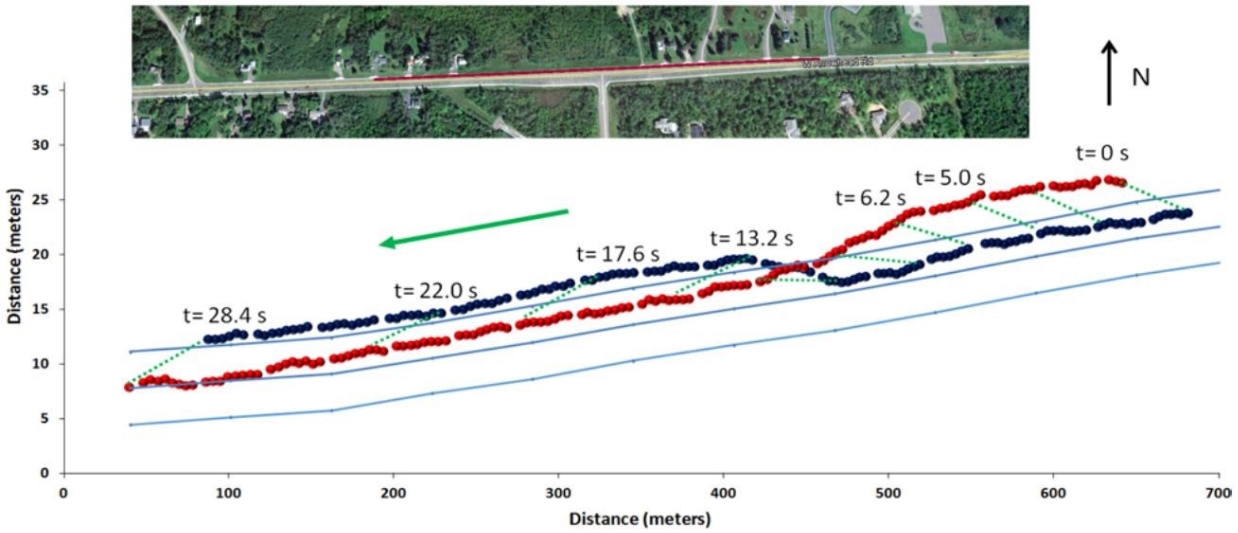

Figure 2.8 GPS error model: The inner circle represents the inherent error of the GPS receiver. The larger circle indicates the overall error. a) The GPS error is non-random b) The GPS error is random.

The lane width of W Arrowhead Rd is about 3.3 meters (measured from Google Earth). The acquired relative trajectories show that the average distance between the two vehicles is about one lane width. The vehicles were travelling almost in the middle of their respective lanes throughout the trial. This shows that relative accuracy of much less than the lane width can be achieved using this method. Please note that the relative distance between the two vehicles is larger before lane switching (right side trajectory in Figure 2.8) as compared to after lane switching (left side trajectory in Figure 2.8). We believe this is due to different inherent errors of the two GPS receivers connected with the DSRC devices present in the two vehicles as illustrated in Figure 2.9, where two GPS readings of the two vehicles each one before lane switching and one after lane switching– are graphically shown. The bigger circle shows the total position error of the GPS receiver from all sources including atmospheric errors and inherent GPS receiver error. Although, the error caused by atmospheric sources is supposed to be same for all nearby GPS receivers, the inherent GPS error will be different for each GPS receiver. The smaller circler represents the inherent GPS receiver's error. We believe that the inherent GPS receiver error vectors of the two GPS receivers of the two vehicles have a net vertical components (Δ) in opposite direction (Figure 2.9) which can explain the differential distance between the two vehicles before and after the lane switching. Please note that net vertical error component means the error component perpendicular to the road direction. The differential distance between the two lanes becomes LW+ 2 Δ before the lane switching and becomes LW - 2 Δ after the lane switching, where LW is the lane width. Please note that in the illustration of Figure 2.9,

radii of inherent errors' circles and the net vertical error components (Δ) of two GPS receivers are assumed to be same but they don't necessarily have to be same for all or any two GPS receivers.

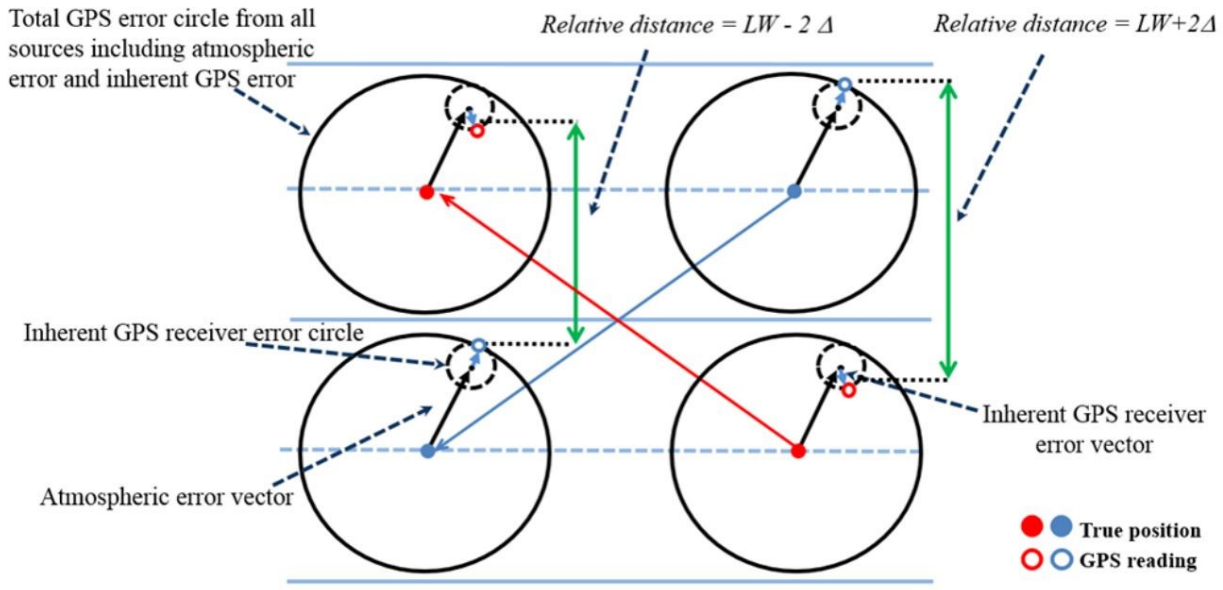

Figure 2.9 The impact of the inherent GPS receiver's error on the relative trajectory accuracy.

2.3.3.2 Lane Merging Scenario

The lane merging scenario field test was also conducted on W Arrowhead Rd. In this trial, the two vehicles started on two adjacent and one vehicle merged into the other lane in the middle of the trial. We used the same Arada Locomate 200 DSRC devices for these tests as well. Please note that we also repeated the tests with Savari S100 DSRC devices but those results are not shown here. The acquired trajectories of the two vehicles using Arada LocoMate 200 devices are shown in the Figure 2.10 in the same format as shown for lane switching scenario in Figure 2.8. The blue dotted lines represent the trajectory of the vehicle which merged on the same lane where the vehicle with the trajectory represented by red dotted lines was travelling.

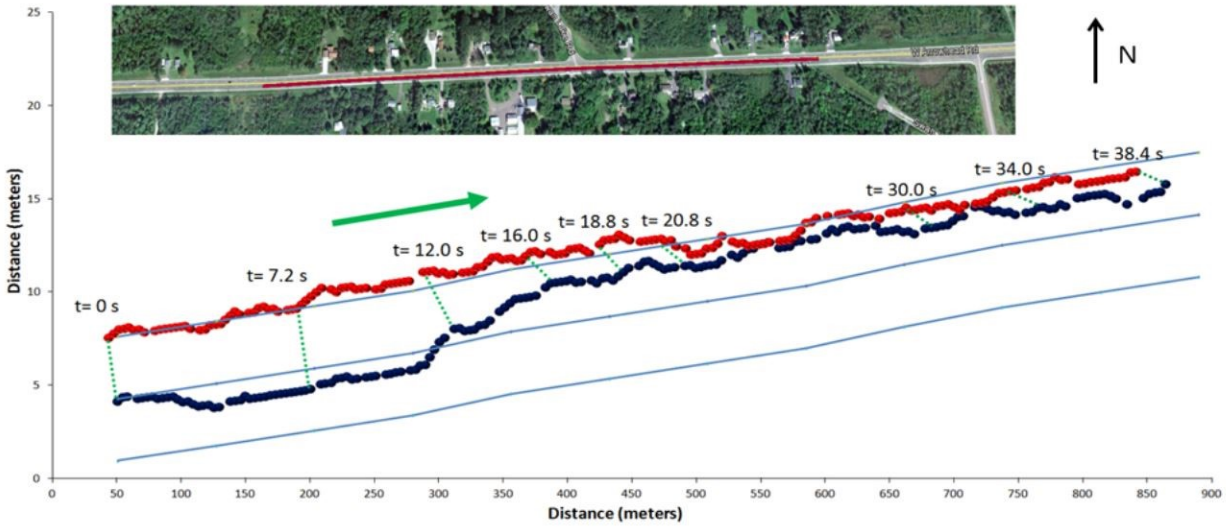

Figure 2.10 Lane-merging field test on W Arrowhead Rd using two Arada Locomate-200DSRC devices.

2.4 IMPLEMENTATION OF THE RELATIVE ACCURACY THEORY

After qualitatively validating the relative accuracy theory, we also accurately quantified the relative GPS positioning accuracy before conducting our road tests using completely developed system. In this section, we will first elaborate the field test in which we statistically characterized the relative GPS positioning error and then give the results of our freeway tests using our system.

2.4.1 Characterization of the GPS relative accuracy

Similar to the trajectory of a single vehicle, which can be obtained by a GPS receiver with a small variance, the relative trajectories of multiple vehicles in close proximity that have their own GPS receivers can also be obtained with comparable variances. Two practical scenarios involving multiple vehicles—merging and changing lanes on freeway—are depicted in 2.11 (left side). In both scenarios, the relative trajectories of surrounding vehicles, if accurately known, can be beneficial in the development of traffic safety applications. Using the GPS error model described above, the relative positions of three vehicles obtained by GPS receivers are shown in 2.11 (right side) at a given time. The estimated GPS position of each vehicle (shown by red dots) will have the same offset from the true position because the net atmospheric and ephemeris error remains the same for all three vehicles, provided they are equipped with GPS receivers of the same model. Therefore, the relative distance between any two vehicles in both scenarios calculated from the estimated positions of the GPS receivers on the two vehicles will have a small variance determined by the mechanical errors of the GPS receivers. An accurate estimate of relative distance between any two vehicles at a given time can lead toward an accurate estimate of the relative trajectories of those vehicles with respect to each other. The accuracy of the relative trajectories needs to be high enough for use in a potential safety application, such as a lane-merge or lane change-assist system, where it is necessary to determine if a neighboring vehicle is in the same or adjacent lane.

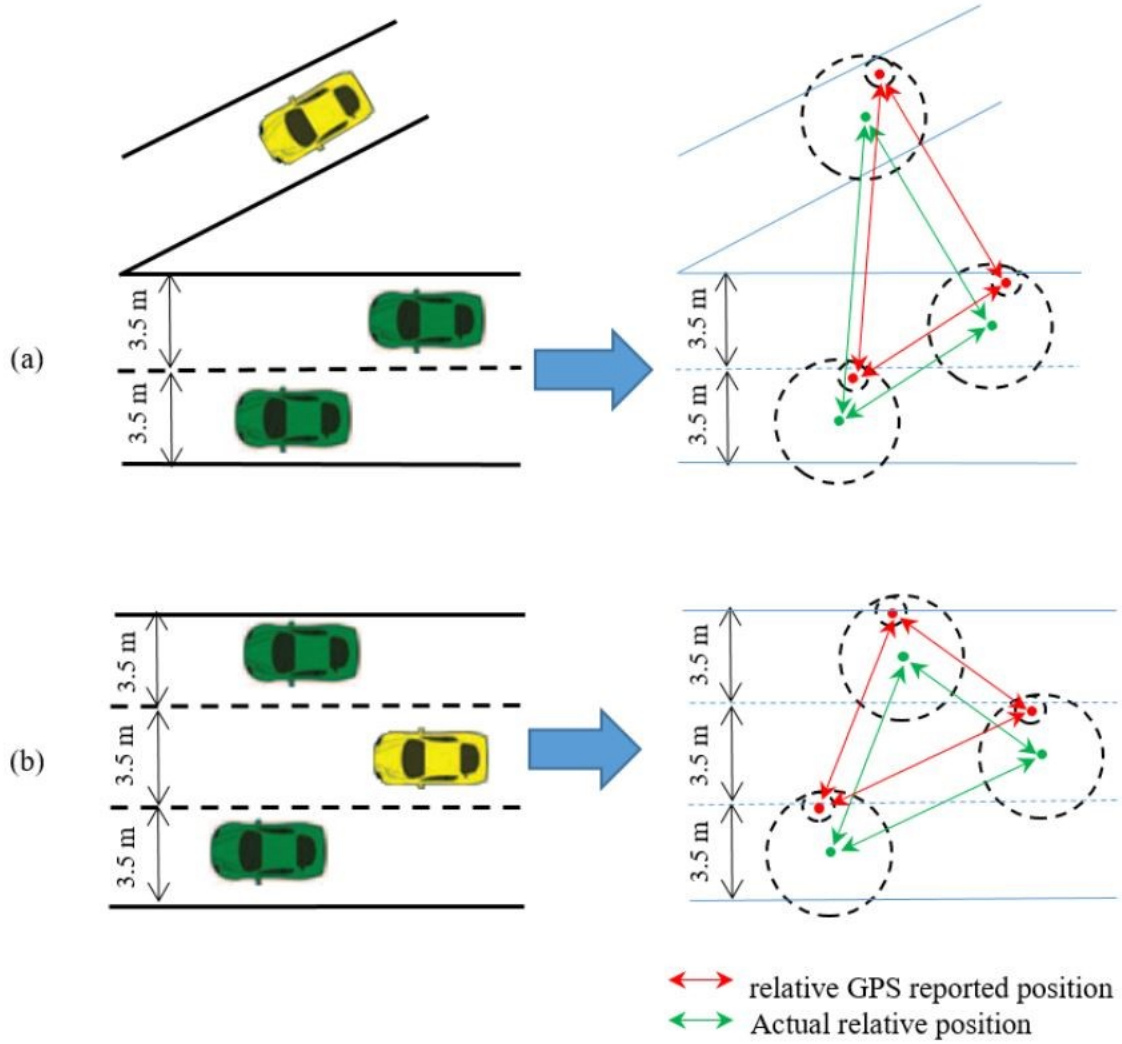

Figure 2.11 Concept of relative GPS accuracy: (a) Lane-merging scenario (b) Lane changing scenario.

2.4.1.1 Test Setup

The relative trajectories of surrounding vehicles can be obtained for any given vehicle on the road provided it can receive the estimated GPS positions of the neighboring vehicles. We used DSRC-based V2V communication to exchange position information among surrounding vehicles that had standard GPS receivers, which allowed GPS position data from neighboring vehicles to be processed in any vehicle to obtain relative trajectories. Before conducting field tests to obtain relative trajectories of multiple vehicles on the road, the relative distance accuracy of the standard GPS receivers built in to the DSRC devices needed to be characterized to determine if it is sufficient to distinguish the neighboring vehicles in the same or adjacent lanes. Therefore, we statistically characterized the relative distance accuracy of the GPS receivers built in to the DSRC devices and later used the same devices to acquire the relative trajectories of multiple vehicles using DSRC-based V2V communication. The built-in GPS receivers use a UBlox LEA-6 chipset, which is specified as having a ± 2m absolute position accuracy with 50 percent circular error

probability (CEP). Using these GPS receivers, we have been able to achieve the relative distance accuracy of ± 0.5m with 95 percent CEP in our field tests. We conducted field tests to statistically evaluate the accuracy of the relative distance obtained by the built-in GPS receivers of the DSRC devices. We installed antennas for three DSRC devices on top of one vehicle at locations A, B, and C, as shown in figure 2.12. A top view of the vehicle used for the field tests is shown in 2.12a, and 2.12b is a top-view schematic of the vehicle showing the three antenna locations (A, B, and C). The three locations formed a right-angle triangle with two shorter legs of length 1m each. We drove the equipped vehicle on I-35 near Duluth, MN, in a round trip between exit #239 and #242 at a speed of about 70 MPH (speed limit) while continuously acquiring GPS position data in all three devices at the rate of 10 Hz.

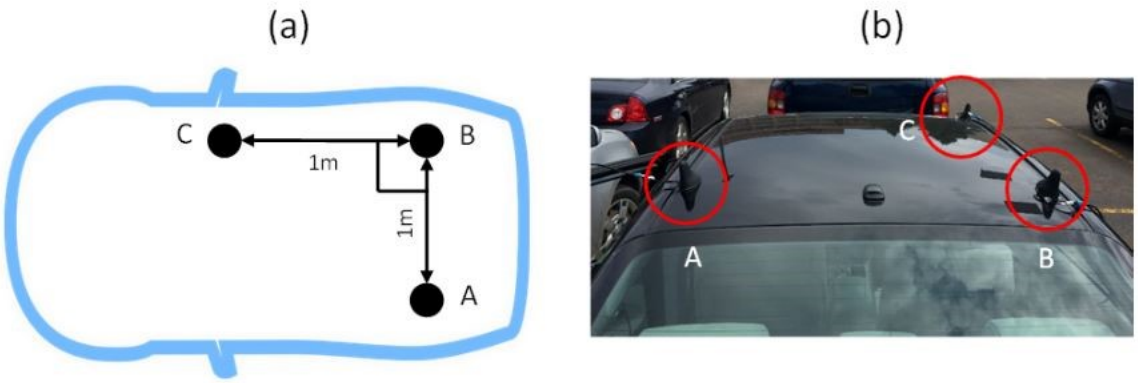

Figure 2.12 The top view of the vehicle used for the field tests with (a) pictorial view and (b) schematic view, showing three installed antennas and their relative locations. The top view of the vehicle used for the field tests with (a) pictorial view and (b) schematic view, showing three installed antennas and their relative locations.

2.4.1.2 Results Analysis

Distance Accuracy

We repeated the round trip six times, exchanging the positions of the antennas at locations A, B, and C after each trip and using all six possible permutations of the three devices. Each round trip produced three distinct sets of acquired GPS positions (one for each GPS receiver at location A, B and C) in terms of longitude and latitude at distinct time intervals synchronized with the GPS satellite time. There were more than 12,000 GPS points in each of the three sets of data (i.e., a net 20 minutes' worth of data with 10 Hz GPS acquisition rate). We then processed the data from all three DSRC devices to calculate three distances (AB, BC, and AC) for each set of three GPS points acquired at the same time because the clock of each GPS receiver was synchronized with the GPS satellite. The calculated average distances of AB, BC, and AC were 1.15, 1.16, and 1.6m, with standard deviations of 0.21, 0.20, and 0.24m, respectively, as shown in Figure 2.13. The calculated average distances of AB, BC, and AC are shown in Figure 2.13 where a circle with a 0.25m radius is drawn at each location (A, B, and C) to indicate the spread of the calculated relative distance because the standard deviation of each calculated distance is less than 0.25m. The variation of the relative distances of AB, BC, and AC is within ± 0.5m most of the time (>95%), as illustrated in the histogram of each segment in 2.13. Furthermore, the histograms show that the maximum spread of each relative distance is within a ± 0.6m limit (1.2m total spread), which is still less than half of the lane width, and therefore, is sufficient to differentiate vehicles on adjacent lanes.

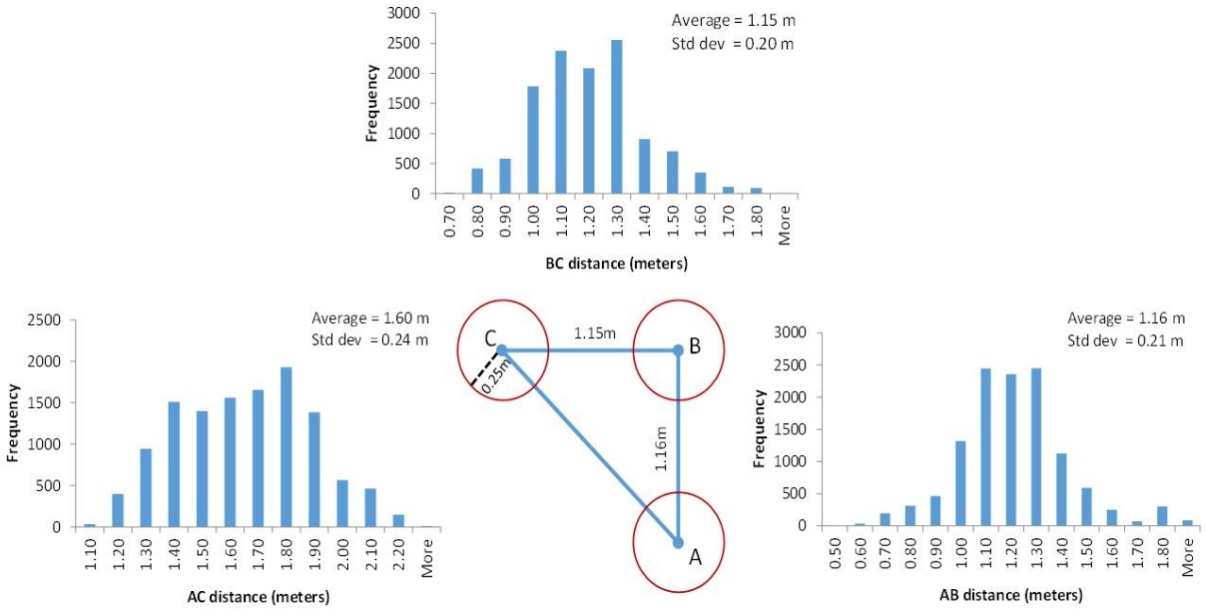

Figure 2.13 Average calculated distances of segments AB, BC, and AC. The histogram of each segment length is shown beside the segment. The average angle ABC is 87.8 degrees.

Although the specified absolute position accuracy of each GPS receiver used was ± 2m with 50 percent CEP, the relative position accuracy between any two GPS receivers was much improved because the net

ephemeris and atmospheric error in absolute position was similar in all three GPS receivers and was therefore canceled out in the relative distance calculation. In our approach to characterize relative distance accuracy, we used standard GPS receivers of the same hardware and firmware model. This was necessary because the post processing of the GPS signal may vary among different GPS chips being used on different DSRC devices. The processing algorithm may also be different among different versions of firmware on the same kind of GPS chip. Furthermore, the GPS receiver's field of view is wide enough to receive signals from more than three or four GPS satellites, which is the minimum number of satellites required for two-dimensional or three-dimensional position calculation, respectively. In such scenarios, unless the post-processing algorithm of multiple GPS receivers is designed to lock to the same set of satellites, it is not guaranteed that the atmospheric and ephemeris errors will remain the same in each GPS receiver—thereby adversely affecting the relative distance accuracy. We experienced this phenomenon only twice during our early field tests when the offset of at least one of the three GPS receivers used was different from the others, indicating that this particular GPS receiver locked to a different set of satellites. In the built-in GPS receivers of our DSRC devices, we did not have any access to modify the GPS receiver firmware to make it lock to a particular set of satellites. However, we did not experience this phenomenon in any of our subsequent field tests, including the tests described in this report.

Direction Accuracy

We also evaluated the directional accuracy for each of the GPS receivers in this field test. We took two consecutive GPS positions (100msec apart in time) for each of the two GPS receivers at locations A and B and calculated individual headings for both, as shown in Figure 2.14a. Figure 2.14b shows the histogram of difference in headings of the GPS receivers at positions A and B for all available data points, covering six possible pairs of three distinct GPS receivers at two locations (A and B). The average and standard deviation of the differential heading is -0.003 degrees and 0.26 degrees, respectively. Both GPS receivers were traveling in the same direction, so the differential heading was expected to be zero. The results show that a standard GPS receiver can estimate the direction of travel with an accuracy of a quarter of a degree which is sufficient for use in a safety application e.g., a lane-change or merge-assist application. This is because a quarter of a degree mismatch between the actual and expected direction of travel of a vehicle traveling at 60 MPH will cause a displacement error of about 11cm in its expected position after one second.

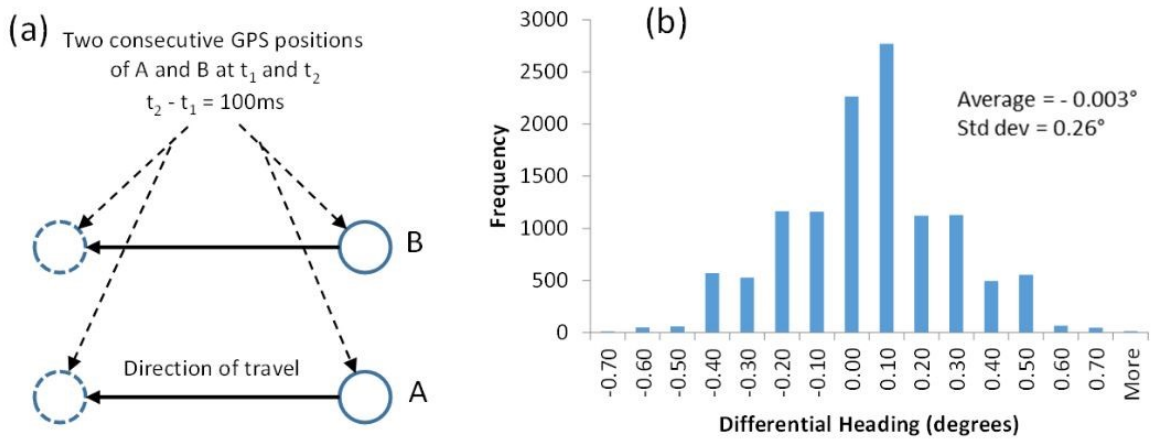

Figure 2.14 (a) The schematic diagram of calculated headings of the two GPS receivers at locations A and B, and (b) the histogram of the differential heading.

CHAPTER 3: RELATIVE LANE IDENTIFICATION AND MERGE TIME CUSHION

3.1 RELATIVE LANE IDENTIFICATION OF VEHICLES USING DSRC BASED V2V

As discussed earlier, the necessary parameters to accurately estimate the merge time cushion in order to facilitate the ramp vehicle to safely merge into the freeway are; Acquiring the accurate relative trajectories of the vehicles, identifying the relative lane and position of the vehicles around the merging junction, identifying the vehicle of concern which could interfere with the merging of the ramp vehicle. In Chapter 2, the authors proposed and demonstrated a method of estimating accurate relative trajectories of surrounding vehicles with lane level resolution using standard GPS receivers and Dedicated Short-Range Communication (DSRC) based Vehicle to Vehicle (V2V) communication. In that work, we exploited the higher accuracy of relative distance between the two GPS receivers in close proximity. The results showed that the relative distance accuracy between the GPS receivers was less than half a lane width.

In this chapter, we will discuss a methodology to estimate the relative lane and position of surrounding vehicles in real time to cost effectively facilitate many critical ADAS functions, including Merge Assist System and other systems such as blind spot detection, overtake, and forward collision warning systems etc. Field tests were performed to evaluate the proposed methodology on a two-lane freeway having sharp curved road sections designed for a maximum degree of curvature for a speed of 120 kmh. The field test results show that the relative lane and position of surrounding vehicles can be identified in real time with 100% accuracy regardless of the degree of curvature of the road as long as the distance between the two vehicles is less than 50 m.

3.1.1 Methodology

The objective of this research is to use DSRC based V2V communication and standard GPS receivers to identify relative lanes and positions of surrounding vehicles in real time, which helps in estimating the merge time cushion. Each vehicle equipped with DSRC equipment transmits and receives Basic Safety Message (BSM) every 100 msec to and from its neighboring vehicles. Among other data, BSM originating from each vehicle at any given time contains its position information in terms of longitude and latitude. When any given vehicle has received position information from its neighboring vehicles, it performs the required calculations as proposed in this report to estimate their relative lane and position with respect to its own. The details of those calculations are described as follows.

The relative lane of any two vehicles on a straight road segment is decided based upon the lateral distance (D_L) between the two vehicles, as shown in Fig. 3.1(a). If the absolute value of D_L ($|D_L|$) is less than ½ of the lane width (LW) of the road, the two vehicles are considered to be in the same lane. And if $|D_L|$ is

more than ½ LW but less than 1½ LW, the two vehicles are considered to be in the adjacent lanes. The sign of D_L helps distinguish the right lane from the left lane.

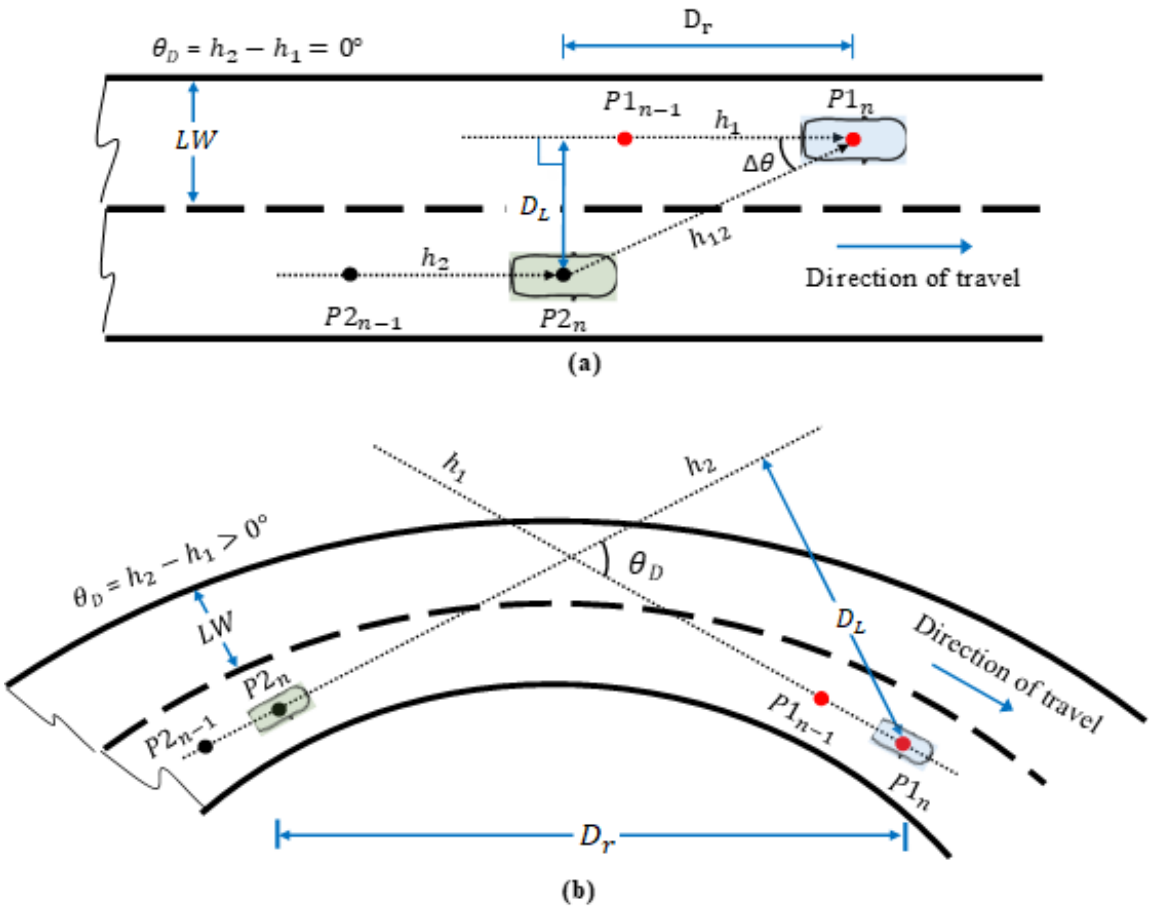

Figure 3.1: Schematic diagram of two vehicles illustrating the concept of relative lane identification on (a) straight road, and (b) curved road. Where $h1$ and $h2$ are the headings of vehicle 1 and vehicle 2, respectively. $P1n$ and $P2n$ are the position coordinate points of vehicle 1 and vehicle 2 at t=n, and $P1(n-1)$ and $P2(n-1)$ are the position coordinate points of vehicle 1 and vehicle 2 at t=n−1. LW is the lane width of the road.

For this research, D_L between any two vehicles is calculated using Point-Line formula in equation (1) which requires at least two distinct rectangular position coordinates of one vehicle: $P1_n(x1_n, y1_n)$ and $P1_{n-1}(x1_{n-1}, y1_{n-1})$, and one position coordinate of another vehicle: $P1_{n-1}(x1_{n-1}, y1_{n-1})$, as shown in Fig 1(a).

$$D_L = \left[\frac{(x1_n - x1_{n-1})(y1_{n-1} - y2_n) - (x1_{n-1} - x2_n)(y1_n - y1_{n-1})}{\sqrt{(x1_n - x1_{n-1})^2 + (y1_n - y1_{n-1})^2}}\right] \quad (1)$$

It should be noted that BSM contains GPS position coordinates in terms of longitude and latitude which is first converted to rectangular coordinates using Universal Transverse Mercator (UTM) conversion method [41] before using eq (1). To correctly identify relative lane of any two vehicles at any given time n, it is

necessary that one of the two position coordinates of one vehicle and the position coordinate of the other vehicle are taken at the same time.

3.1.1.1 Curvature error and its estimation

The above method precisely calculates D_L only when the two vehicles are on a straight road segment which can be differentiated from a curved road segment by calculating the differential heading (θ_D) between the two vehicles at any given time. If θ_D is negligibly small the two vehicles are considered to be on a straight road segment regardless of their relative distance (D_r) from each other, as shown in Fig. 3.1(a). However, when the two vehicles are on a curved road segment, θ_D is no more negligible as illustrated in Fig. 3.1(b), where the two vehicles are shown on a curved road segment occupying the same lane. Although on a curved road segment (Fig. 3.1b) the true D_L between the two vehicles should be less than ½ LW because they occupy the same lane, the calculated D_L between the two vehicles appears to be larger than LW. Hence, D_L calculated using the method described above can no longer be used as such for relative lane identification. Therefore, it is necessary to first estimate the increase in D_L to adjust the calculated D_L between the two vehicles before estimating their relative lane.

The increase in D_L depends upon the curvature of the road and can be estimated using θ_D and D_r between the two vehicles. For simplicity, the increase in D_L between the two vehicles is termed as curvature error (C_e) in this paper and can be estimated using eq (2).

$$C \quad D \quad n\left(\theta \quad\right)$$

C_e is proportional to both θ_D and D_r. The absolute value of C_e ($|C_e|$) is plotted as a function of D_r for 2, 4 and 6 degrees of θ_D in Fig. 3.2(a), and as a function of θ_D for 40, 80 and 120 m of D_r in Fig. 3.2(b). For a straight road segment when θ_D between the two vehicles is small, $|C_e|$ remains small even when the two vehicles are far from each other. However, for a curved road when θ_D between the two vehicles is large, $|C_e|$ can be much larger even when the two vehicles are not far from each other. As can be seen from Fig. 3.2, $|C_e|$ can be much larger than LW especially for sharper curves i.e., large θ_D even when D_r between the two vehicles is relatively small.

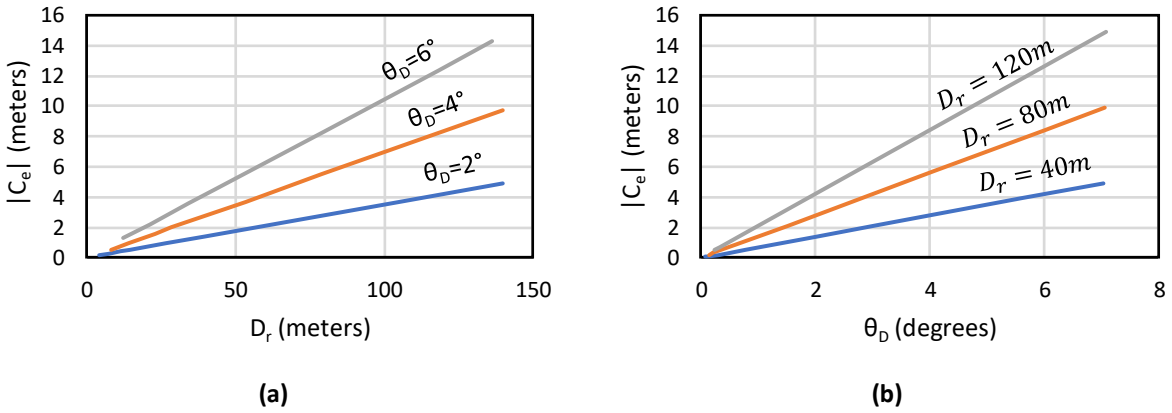

Figure 3.2 Absolute value curvature error (a) as a function of Dr for fixed values of θD and (b) as a function of θD for fixed values of Dr.

Using eq (2), C_e can be estimated by calculating θ_D and D_r between any two vehicles at any given time, for any road segment regardless of the degree of curvature of the road. Once C_e is estimated, it can be subtracted from the calculated D_L to determine the effective lateral distance (D_L'). Instead of using D_L which works well only on a straight road segment, D_L' can be used to identify the relative lane between the two vehicles on any road segment regardless of the curvature of the road. Using D_L', the relative lane decision for same, right and left lanes is made using equations (3), (4), and (5), respectively. Although eq (4) and (5) are for the adjacent lanes, the boundaries of D_L' can be extended in these equations to estimate next to adjacent relative lanes on both right and left sides. It should be noted that for this research, LW was assumed to be 3.6 meters (12 feet) for the freeway lane width [42].

3.1.1.2 Relative position identification (Trailing ahead or behind)

$$-LW \quad D \quad -LW$$

$$-LW \quad D \quad -LW \qquad ( )$$

$$-LW \quad D \quad -LW$$

In addition to identifying the relative lane of surrounding vehicles, the relative position of the vehicles is also vital in many ADAS functions, such as blind spot and overtake warning systems etc. Typically, a blind spot warning system needs to estimate if another vehicle is traveling behind it at a short distance in the adjacent lane. Similarly, an overtake warning system would need to estimate if another vehicle is speeding up from behind at a critical distance in order to issue a warning.

To determine if a given vehicle is trailing ahead or behind the other vehicle, heading between the two vehicles (h12), and the heading (h1) of the other vehicle, as illustrated in Fig. 3.1(a), are needed. With those two headings, Δθ (Fig. 3.1a) is calculated using (6). If Δθ > 90 degrees, then the given vehicle is ahead of the other vehicle and if Δθ < 90 degrees, then the given vehicle is behind the other vehicle.

$$\Delta\theta \quad h \quad h$$

3.1.1.3 Precision in heading calculation

It is important to mention that the precision in heading calculation is critical for relative lane estimation. Heading of each vehicle is calculated by using at least two position coordinates estimated by standard GPS receivers which is susceptible to error and noise [43]. Therefore, to improve the accuracy of calculated heading and hence reliability of the proposed system, a rigorous method is used to estimate the headings of the two vehicles. Heading of each vehicle at any given time is calculated using five consecutive position coordinates instead of two. The heading of each vehicle at the most current position (P_n) is calculated using most recent 5 consecutive position coordinates (P_n, P_{n-1} … P_{n-4}) as shown in Fig. 3.3. The vehicle heading is taken as the average of the two headings calculated between P_{n-1} and P_{n-3}, and P_{n-4} and P_n. Similarly, D_r between the two vehicles at their current positions is calculated as the distance between the middle of the 5 points, i.e., P_{n-2} of both the vehicles. Subsequently, D_L in any given vehicle is calculated by taking the average of the two lateral distances calculated using one position coordinate P_{n-2} of the given vehicle and the two position coordinates of the other vehicle, first using P_n and P_{n-4}, and then using P_{n-1} and P_{n-3} (Fig. 3.3).

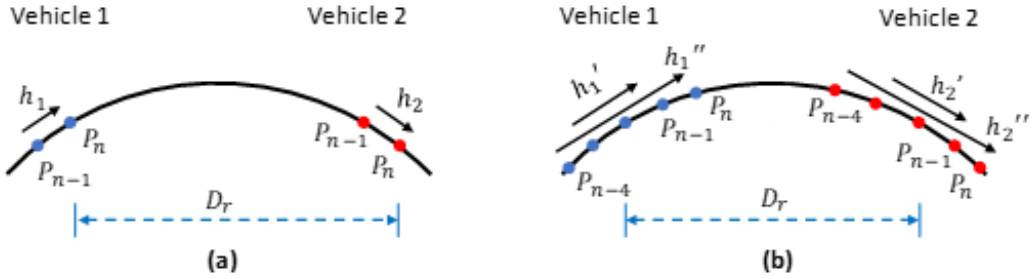

Figure 3.3 (a) Schematic illustration of finding heading of each vehicle using (a) conventional 2-Pointmethod, and (b) 5-Pointmethod.

3.1.2 Field Tests

To evaluate the methodology described above to identify relative lane and position of surrounding vehicles in real time, field tests were performed on a freeway having both straight and curved segments. Two vehicles were used in the road test. Each of the two vehicles was equipped with DSRC equipment and a standard GPS receiver.

Field tests were conducted between Exit #245 and #249 on I-35 in Duluth, MN, which is a two-lane Freeway. Both vehicles were driven back and forth between the two exits, a total of six times (12 runs) occupying a different lane and/or position each time. In the first two trials (4 runs), both vehicles occupied the same lane (right lane) with relative position of vehicle 1 being switched from trailing ahead in the first trial to trailing behind in the second trial. In the remaining four trials, both vehicles occupied different lanes with their relative lane and/or position being changed each time. In each of the total 12 runs of 6 trials, both vehicles travelled ~6.5 km one way on the freeway while D_r between them was varied between 5 to 150 m, maintaining their relative lane and position with respect to each other.

While travelling on the road, both vehicles exchanged BSMs with each other and performed calculations in real time to determine relative lane and position of the other vehicle with respect to its own. The results were displayed in real time on a laptop computer in each vehicle interfaced with the DSRC device. The typical screen shots of the two laptop screens displaying real-time results in two vehicles are shown in Figure 3.4, where the right screen shot is from the vehicle traveling ahead of the other vehicle on the right lane, and the left screen shot is from the vehicle traveling behind on the left lane. The real-time results not only show the relative lane and position of the vehicle but also D_r which was helpful to maintain the desired distance between the two vehicles during the trials. In each of the 6 trials (12 runs), the two vehicles travelled a round trip of about ~13 km and the relative lane and position of the two vehicles was maintained in both directions of travel in each trial. Both vehicles exchanged BSMs and performed necessary calculations to identify relative lane and position of the other vehicle every 100 msec. The average speed of both vehicles was varied between 110 km/h and 120 km/h so it took about 200 seconds to cover 6.5 km each way in any given run. Therefore, in any given run, a decision about relative lane and position of the other vehicle was repeated about 2,000 times producing a total of about 24,000 set of calculations or decisions in all 12 runs.

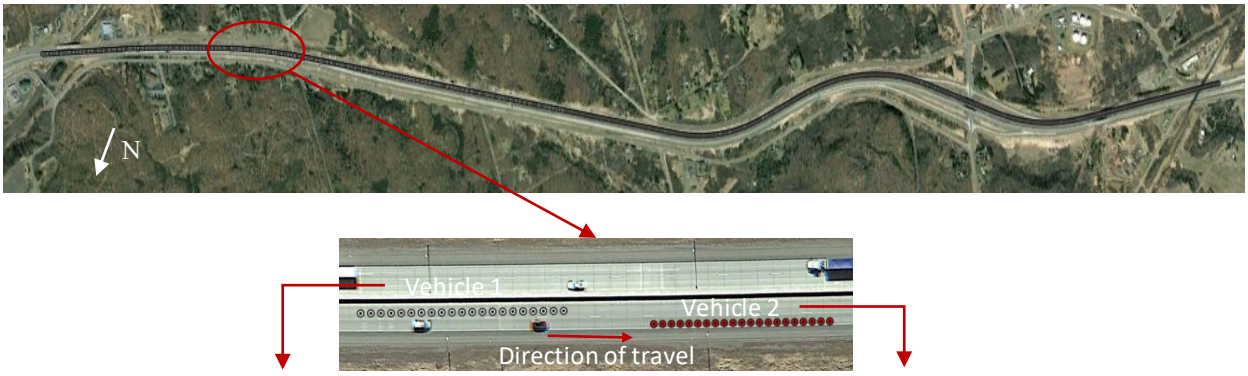

Relative Position	Relative Lane	Relative Distance (meters)
Ahead	Right	123.789
Ahead	Right	123.006
Ahead	Right	122.598
Ahead	Right	122.179
Ahead	Right	121.778
Ahead	Right	121.352
Ahead	Right	120.907
Ahead	Right	120.495
Ahead	Right	120.040
Ahead	Right	119.589
Ahead	Right	119.130

Relative Position	Relative Lane	Relative Distance (meters)
Behind	Left	123.789
Behind	Left	123.006
Behind	Left	122.598
Behind	Left	122.179
Behind	Left	121.778
Behind	Left	121.352
Behind	Left	120.907
Behind	Left	120.495
Behind	Left	120.040
Behind	Left	119.589
Behind	Left	119.130

Figure 3.4 The corresponding road map where the field tests were performed is shown at the top. A zoomed-in portion of the road is shown in the middle along with a few trajectory points of the two vehicles in one of the field tests. The bottom two pictures are the screenshots of the two laptops in vehicle 1 and 2 showing the relative position and lane of the other vehicle with respect to its own in real time.

In each set of calculations; both vehicles, upon receiving a new position coordinate from each other, calculate D_L, θ_D, D_r and C_e as explained in methodology section. Using D_L and C_e, D_L' is calculated which is used to decide the relative lane of the other vehicle according to the rules described in methodology

section (equations 3 - 5). After making decision about relative lane, each vehicle also performs necessary calculations as explained earlier to determine relative position of the other vehicle.

3.1.3 Results and Discussion

In each of the 12 runs, both vehicles performed calculations followed by a decision about the relative lane and position of the other vehicle every 100 msec. The necessary set of calculated parameters to be used in (6) to determine the relative position of the vehicle are much less prone to noise as long as D_r between the two vehicles is more than a few meters. As a result, at every time instance of all 12 runs, the decision of both vehicles to determine relative position of each other was 100% accurate because the relative distance between the two vehicles at any given time was at least 5 m during the entire field tests. Therefore, in this section, the detailed calculation results for relative position identification will not be discussed any further. On the other hand, the calculated parameters especially θ_D, needed to be used in (2) to determine the relative lane are much more sensitive to noise. Therefore, at some time instances of the 4 out of 12 runs of the field tests some erroneous decisions in relative lane determination were observed. There were a total of 314 errors observed in those 4 runs, most of which occurred on the curved section of the road especially when the two vehicles were far from each other. However, in the remaining 8 of the 12 runs, the relative lane decision was 100% accurate. The accuracy of lane estimation is calculated as the percent ratio of the number of erroneous decision and the total number of decisions made.

3.1.3.1 Example 1: Trial with only few errors

A typical set of calculations of one of the two vehicles is shown in Figure 3.5(a) where D and θ are plotted versus time travelled, for one of the 4 runs with errors. In this run, D between the two vehicles varied between 30 and 100 m and θ varied between -2 and +2.5 degrees as evident from Figure 3.5(a). The map of the road section where the two vehicles traveled during the field tests is also shown on the top of the Figure 3.5 to provide context of travelling position of the two vehicles. As θ between the two vehicles is directly correlated with the degree of curvature of the road as well as D , it is larger when the vehicles are on curved section of the road (higher degree of curvature) especially when D is also large. In Figure 3.5(b), corresponding C is plotted versus time showing that C is large when θ is large and small when θ is small. As discussed earlier, C is subtracted from D to determine D which is used to decide the relative lane of the two vehicles. The corresponding D is also shown versus time in Figure 3.5(b). In this run, both vehicles were travelling on the same lane, so D should be between ±1.8 m because LW was taken to be 3.6 m. As seen in Figure 3.5(b), D is between the bounds of ±1.8 m at all time instances (~2000) except for 4 times around 16 seconds' time mark when it slightly crosses the upper bound of threshold (1.8 m) making a wrong decision on relative lane. Those 4 erroneous decisions are also highlighted in Figure 3.5(a) with a grey mask.

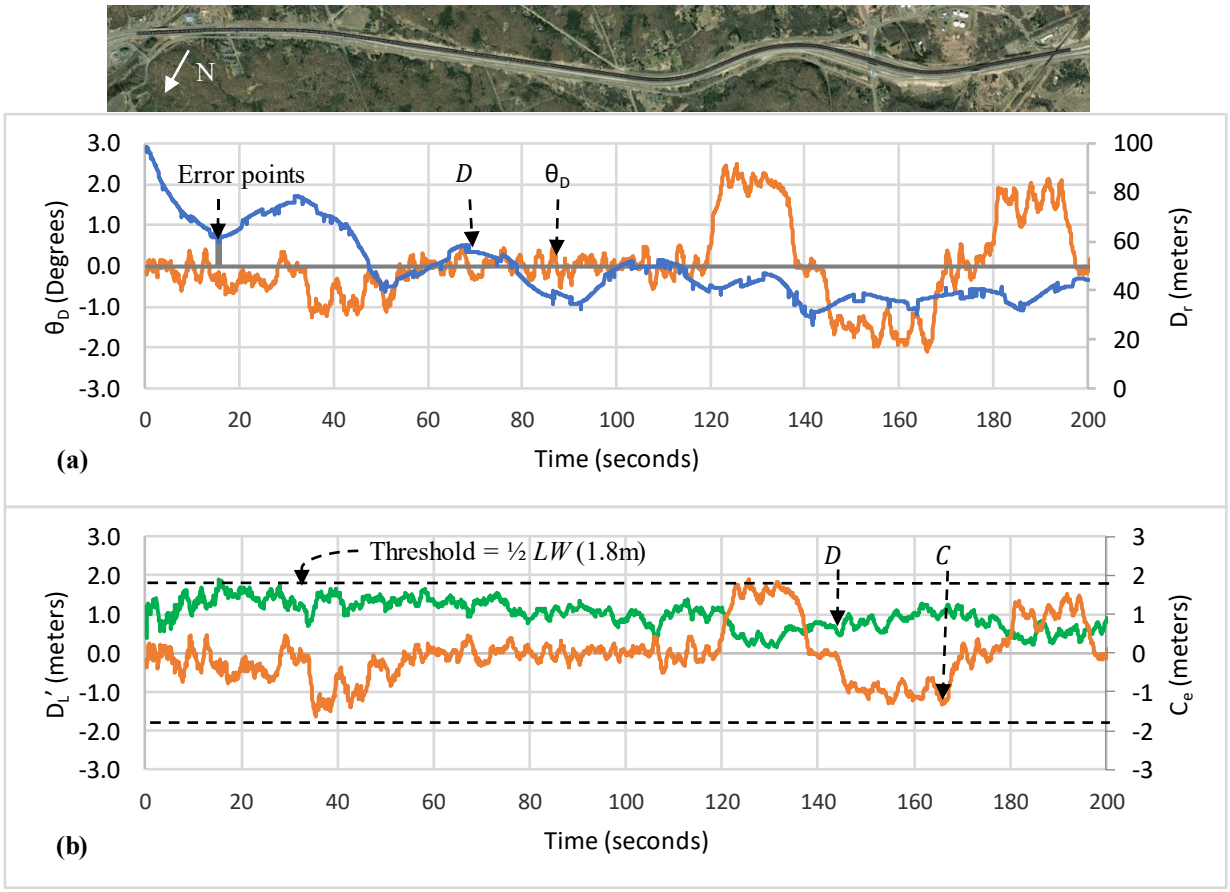

Figure 3.5 (a) θD and Dr vs time and (b) Ce and DL' vs. time, for field test run #1 where many erroneous lane decisions were observed. The erroneous decisions are shown with grey mask in (a). The corresponding road map of the field test is shown on the top of the figure.

3.1.3.2 Example 2: Trial with more errors

Similar to the run in Figure 3.5 where 4 errors occurred, in another run out of total 4 runs with errors, only 8 errors were experienced. Although, these two runs had only a few errors (4 and 8), the remaining two out of the 4 runs with erroneous decisions had relatively large number of continuous errors. For one of those two runs, the calculated D and θ between the two vehicles versus time is shown in Figure 3.6(a). In this run, D between the two vehicles was varied between 20 and 120 m whereas θ between the two vehicles varied between -4 and +5 degrees. The peak values of θ occurred around the curved section of the road where D between the two vehicles was also large (>80 m), as can be seen in Figure 3.6. The larger values of θ resulted in much larger values of C as shown in Figure 3.6(b), where corresponding C is plotted versus time. In this run, C varies between -6 m and +8 m taking higher values on the curved sections of the road where both D and θ are larger, as can be seen from the corresponding map of the road on the top of the Figure 3.6. Along with C , D is also plotted versus time in Figure 3.6(b). The two vehicles were traveling on two adjacent lanes in this run, so D should be either between 1.8 to 5.4 m or -5.4 to -1.8 m for correct lane identification. The threshold lines are shown in Figure 3.6(b) to illustrate that D crossed the threshold bound for relatively longer periods of time resulting in erroneous relative

lane decision. This occurs on the sharper curved sections of the road when D between the two vehicles is also large (> 80m) so that C becomes too large (> 6m) to be corrected using proposed methodology.

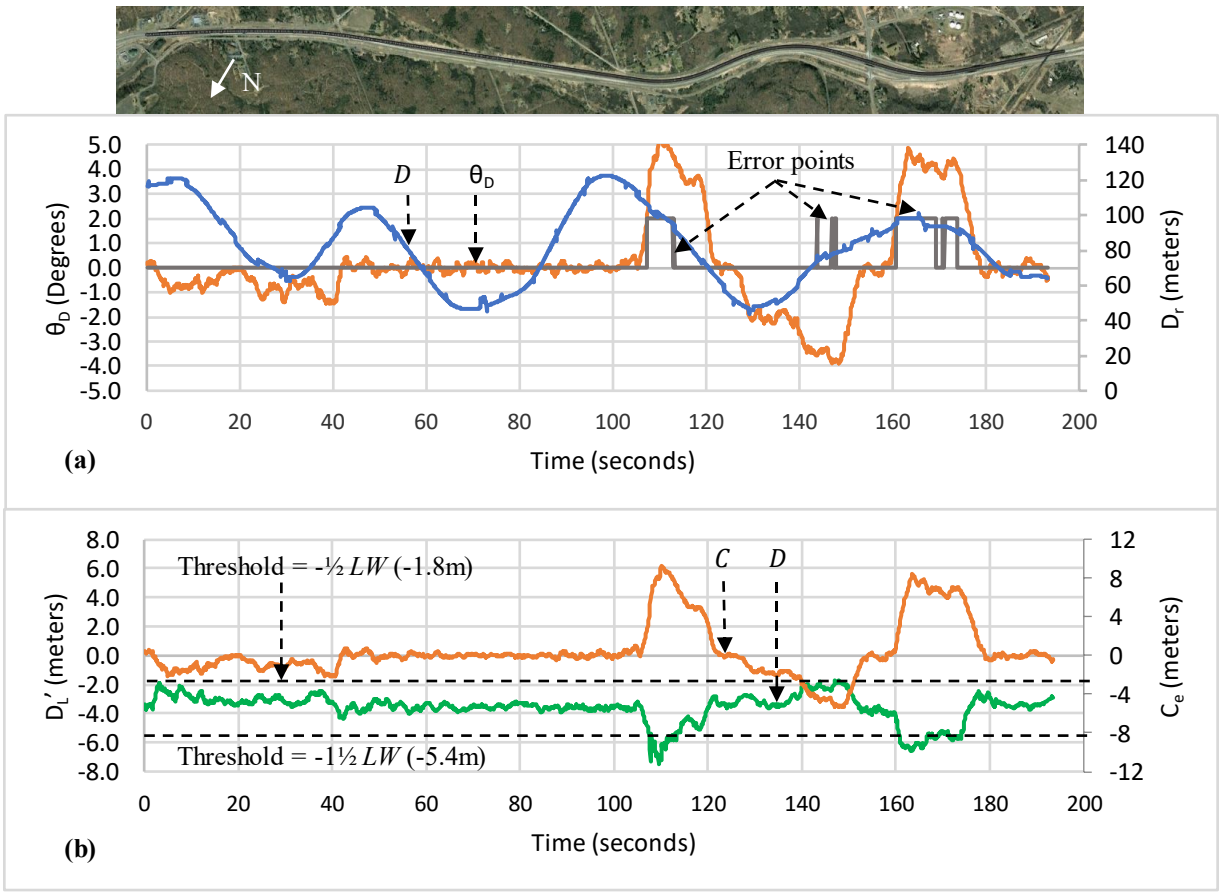

Figure 3.6 (a) θD and Dr vs time and (b) Ce and DL' vs. time, for field test run #5 where many erroneous lane decisions were observed. The erroneous decisions are shown with grey mask in (a). The corresponding road map of the field test is shown on the top of the figure.

3.1.3.3 Error analysis

The relative lane identification error was highly correlated with $|C_e|$ with likelihood of error increasing with larger values of $|C_e|$. The values of $|C_e|$ ranged from almost zero for the straight road section to up to 10 m for the curved road sections during all 12 runs. To find the boundaries of reliable relative lane decision, the range of values for both D_r and θ_D for fixed values of $|C_e|$ were calculated and are shown in a contour plot in Figure 5(a) where D_r is plotted versus θ_D for 1, 2, 3, 4, 5, and 10 m of $|C_e|$. Similarly, the acquired values of $|C_e|$ during the field tests, in terms of its corresponding D_r and θ_D, from all ~24,000 time instances in 12 runs are also superimposed on the contour plot of Fig. 3.7(a). For all except 314 time instances, the calculated value of C_e resulted in correct relative lane identification of the two vehicles. For those 314 time instances resulting in erroneous relative lane identification, the acquired values of $|C_e|$ are shown in a similar contour plot in Fig. 3.7(b). As can be seen from Figure 3.7(b), most of the time the erroneous lane decision was made where the value of $|C_e|$ was quite large due to the two test vehicles

being on the curved sections of the road resulting in a large value of θ_D (>3 degree) where D_r is also large (>80m).

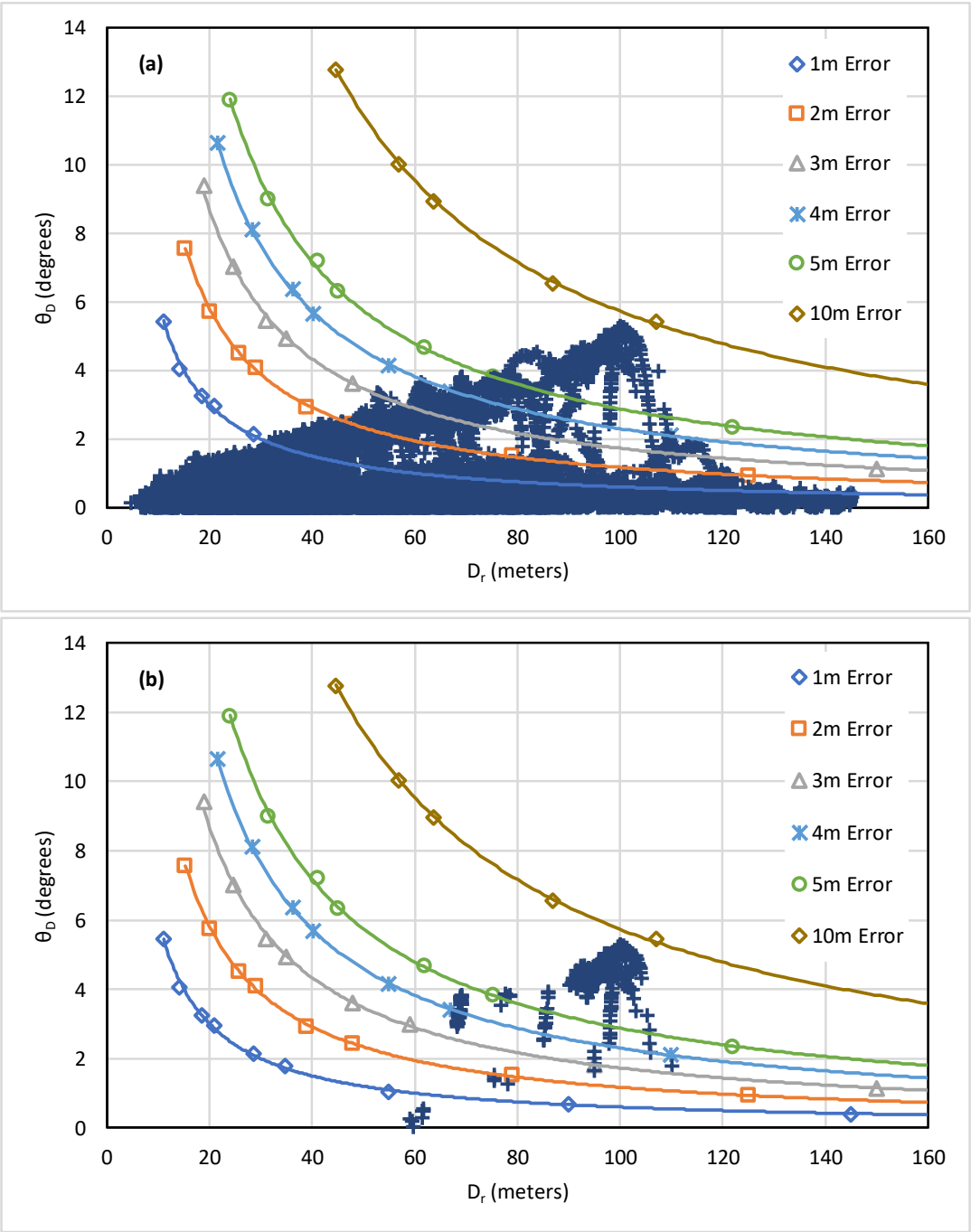

Figure 3.7 The contour plot of θ_D vs. D_r for fixed values of calculated |C_e | (1m, 2m 3m, 4m 5m, and 10m). The contour plot of θ_D vs. D_r for fixed values of calculated $|C_e|$ (1m, 2m 3m, 4m 5m, and 10m). All acquired values of $|C_e|$ in real time during the entire duration of field test are superimposed in (a), and only those acquired values of $|C_e|$ where an erroneous relative lane decision was made are superimposed in (b).

Fig. 3.7(b) also shows that there was no erroneous decision in relative lane identification in all 12 runs regardless of the degree of curvature of the road when the D_r was less than 50m. The overall accuracy of relative lane decision for all 12 runs is summarized in Table 1 for different values of D_r. The accuracy decreases when D_r increases on curved sections of the road resulting in larger values of $|C_e|$. However, for straight sections of the road, values of $|C_e|$ remain small even for larger values of D_r resulting in improved accuracy. Therefore, a limit on the value of $|C_e|$ may be imposed to improve accuracy of lane identification to accommodate curved sections of the road where $|C_e|$ becomes large. For example, for up to 150 m D_r, the overall accuracy is 98.67% without limiting $|C_e|$ but can be improved to 99.71%, and 99.96% by limiting $|C_e|$ to 5 and 3 m, respectively (Table 1). It should be noted that by limiting $|C_e|$, relative lane decision would not be performed in some cases in which $|C_e|$ is larger than the specified limit. However, for those safety applications, for which the relative lane and position of the surrounding vehicles is needed only within a small relative distance of each other, limiting $|C_e|$ will not exclude many cases of practical interest.

3.2 MERGE TIME CUSHION

Merge time cushion is defined as the time required for the vehicle in the right most lane of the freeway to arrive at the common merging point which could potentially interfere with the merging of the ramp vehicle. DSRC equipped vehicles travelling on the freeway and on the merging ramp will periodically communicate important traffic parameters such as their location, direction of travel, and speed, to each other. Using that information, the relative trajectories of all DSRC equipped vehicles travelling on the freeway will be acquired and then processed in real time to identify their relative lane and position. Once the relative lane and position of the vehicles traveling on the freeway are identified, a merge time cushion will be estimated which could potentially be used as an important parameter to develop a merge assist application.

The idea of merge time cushion is shown in Figure 3.8, where one vehicle is shown at a merge junction of a freeway and two more vehicles are shown on the main freeway. Once the DSRC communication is established between the vehicles on the main freeway and the vehicle on the merge junction, and relative positions of the vehicles are calculated in the DSRC device of the vehicle on the merge junction, it will be determined which vehicle is on the right most lane of the freeway which could interfere with the merging of the vehicle on the merge junction. Once lane determination is confirmed, using the speed of the vehicle on the right most lane, a merge time cushion will be estimated which is the time for the vehicle on the right most lane to reach to the common merging position, M, of the merging vehicle and the vehicle on the right most lane as shown in Figure 3.8. The merge time cushion will be updated continuously in real time and it may slightly change depending upon the speed of the vehicle on the rightmost lane of the freeway and/or the geometry of the merging ramp. Please note that if there is only one vehicle traveling towards the merging junction on the freeway, it will be considered to be in the right most lane. Furthermore, the vehicle leading ahead in the right most lane towards the merging junction will be chosen for merge time cushion calculation.

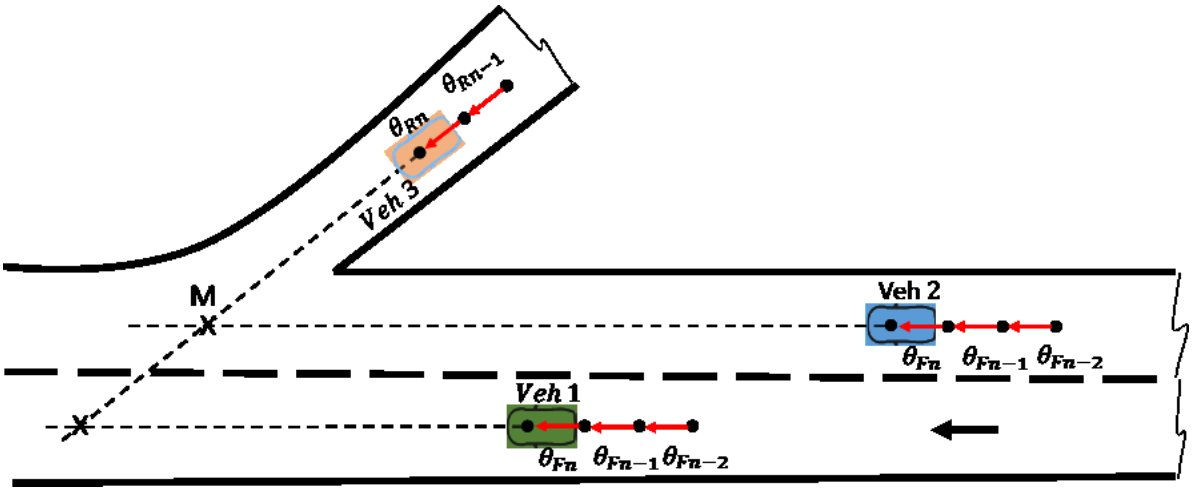

Figure 3.8 Graphical representation of merge time cushion calculation, where the ramp vehicle merges into the freeway in a straight path. 'M' is the common merging point of vehicle 2 and vehicle 3.

There are typically two distinct scenarios in calculating merge time cushion w.r.t the geometry of the freeway ramp. Figure 3.8 illustrates a scenario when the vehicle on the merging ramp merges into the freeway in a relatively straight path (case 1), whereas Figure 3.9 shows a scenario where the freeway ramp is a sharp curve and vehicle merges into the freeway in a curved path (case 2). In figure 1 θ_{Rn} and θ_{Rn-1} are the headings of the vehicle traveling on the ramp. Similarly, θ_{Fn} and θ_{Fn-1} are the headings of the vehicles travelling on the freeway. 'M (P_x, P_y)' is the merging point where the trajectories of the vehicles travelling on the ramp and freeway intersect each other.

$$\Delta\theta_R = \theta_{Rn} - \theta_{Rn}$$

$$\Delta\theta_F \quad \theta_{Fn} - \theta_{Fn}$$

To distinguish between case 1 and case 2, we calculate $\Delta\theta_R$. If $\Delta\theta\_R \simeq 0°$ or less than a certain threshold, we consider that the vehicles is travelling in a straight path (case 1). Similarly, if $\Delta\theta_R$ > threshold, we consider that the vehicle is travelling on a curved path (case 2).

Case 1:

Calculating merging point '$M\ P_x, P_y$ ': As the two vehicles are travelling in a relatively straight path, their merging point can be estimated by calculating where the two straight lines intersect. This can be done by using Line-Line intersection equation (10).

$$P_x \quad \frac{(x\ y\ -x\ y\quad x_3 - x\qquad x_3 y\ -x\ y_3)(x\ -x}{x\ -x\quad y_3 - y\qquad x_3 - x\ )(y\ -y}$$

$$P_y \quad \frac{x\ y\quad x\ y\quad y_3\quad y\qquad x_3 y\quad x\ y_3\quad y\quad y}{x\quad x\quad y_3\quad y\qquad x_3\quad x\quad y\quad y}$$

Merge time cushion or Time to M (TTM): Once 'M' is calculated we can calculate the merge time cushion or TTM by calculating the distance between the vehicle traveling on the freeway and the common merging point M (DTM), and divide it by its speed.

$$Merge\ t\ me\ cu\ h\quad n\ or\qquad DT\quad /Speed$$

Case 2:

As the vehicle travelling on the ramp is not travelling in a straight path (Figure 3.9), its trajectory cannot be extended to accurately estimate 'M'. However, most looped ramps have a straight section at the end of the ramp for the merging vehicles to accelerate and merge into the freeway. More research needs to be done to study and test the geometry of wide range of ramps. For now, we have noticed that most looped ramps start transitioning into a relatively straight road when θ θ_F θ_R 90. Therefore, the same method used in case 1 can be applied but with some added adjustments. For example, in the case of figure 3.9, after θ is < 90 the ramp starts transitioning into a relatively straight path. However, Distance to 'M' (DTM) of the freeway vehicle is estimated less than the actual DTM. As illustrated in figure 3.9, after each point the estimated DTM gets closer and closer to the actual distance. Therefore, by gathering enough data, θ and the difference between estimated DTM and actual DTM can be used to form a trendline which can be used to adjust the estimated DTM. Once DTM is adjusted, it can be used to calculate the merge time cushion.

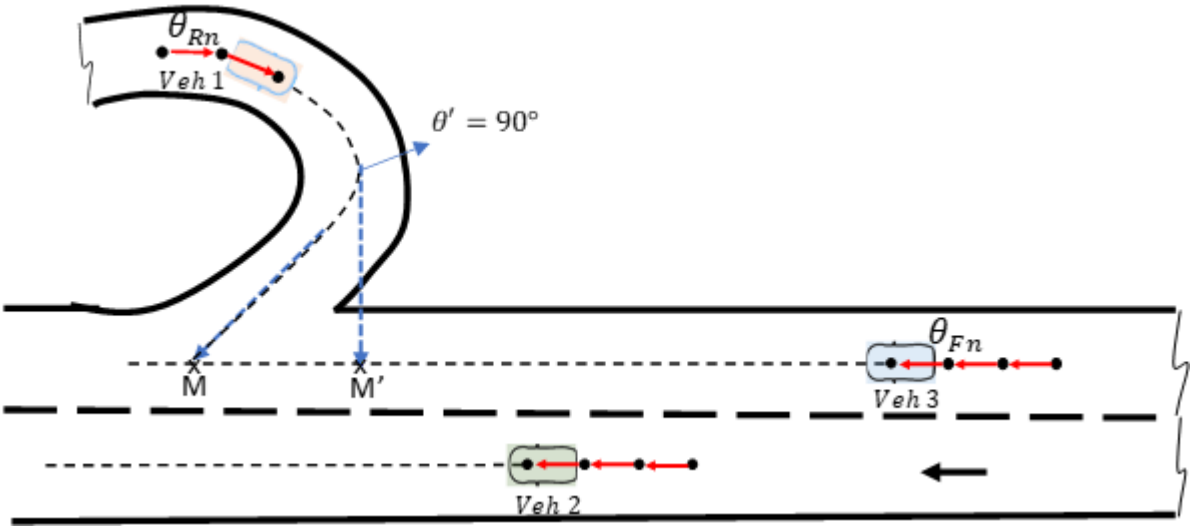

Figure 3.9 Graphical representation of case 2, where the ramp geometry is loop-shaped.

CHAPTER 4: CONCLUSION AND FUTURE WORK

In this report, a methodology is presented to estimate the merge-time cushion using standard GPS and DSRC-based V2V communication. The merge-time cushion can potentially be used by the driver of the ramp vehicle to safely merge into the freeway. A methodology to accurately identify the relative lane and position of surrounding vehicles in real time using standard GPS receivers and DSRC-based V2V communication is also presented. The identification of relative lane and position benefits could not only be used in a merge assist system but also in many other ADAS functions such as blind spot detection, overtake warning system, etc. Field tests were performed on a freeway with a variety of curved road sections to evaluate the proposed lane identification methodology. The results of field tests show that the relative position of the surrounding vehicles in terms of which vehicle is trailing ahead or behind can be identified without any errors as long as the relative distance between them remains at least a few meters. On the other hand, the accuracy of relative lane identification was not 100% in all cases, especially when the relative distance between the two vehicles was large on curved road sections. Most of the errors occurred where the road segment had sharp curves and the relative distance between the two vehicles was >80 m and no errors were observed when the distance between the two vehicles was <50 m, regardless of the degree of curvature of the road.

To estimate the merge-time cushion, two distinct merging scenarios and their solution are presented based on the geometry of the road. However, more tests need to be conducted to test the performance of the proposed methodology. For future work, field tests should be conducted to estimate the merge-time cushion in real time, where one vehicle will be travelling on the freeway entrance ramp and (at least) two more vehicles will be travelling on the main freeway. The two vehicles on the main freeway will travel toward the merging point, and the ramp vehicle will follow to merge into the freeway at the same time. Once the DSRC communication is established between the vehicles on the main freeway and the vehicle on the freeway ramp, and relative positions of the vehicles are calculated in the DSRC device of the vehicle on the merge junction, it will be determined which vehicle is on the right-most lane of the freeway that could interfere with the merging of the vehicle on the merge junction. Once lane determination is confirmed, using the speed of the vehicle on the right-most lane, a merge-time cushion will be estimated, which will be shown to the driver of the ramp vehicle on the tablet screen in the form of how much time is needed for the right-most vehicle to reach to the common merging point. The merge-time cushion will be updated continuously in real time and it could change slightly depending on the speed of the vehicle on the right-most lane of the freeway and/or the geometry of the merging ramp. Please note that if there is only one vehicle traveling toward the merging junction on the freeway, it will be considered to be in the right-most lane. Furthermore, the leading vehicle in the right-most lane toward the merging junction will be chosen for merge-time cushion calculation.

REFERENCES

1) J. Barbaresso, G. Cordahi, D. Garcia, C. Hill, A. Jendzejec, Karissa Wright. (2014). ITS Strategic Research Plan 2015-2019. Retrieved from http://www.its.dot.gov/strategicplan.pdf.
2) A.T. McCartt, V.S Northrup, RA Retting. (2004). Types and characteristics of ramp-related motor vehicle crashes on urban interstate roadways in Northern Virginia. *Journal of Safety Research*, 35, 107– 114.
3) B. N. Janson, W. Awad, J. Robles, J. Kononov, & B. Pinkerton. (1998). Truck accidents at rreeway ramps: Data analysis and high-risk site identification. *Journal of Transportation and Statistics, Volume 1, 75 – 92.*
4) C. Lee, B. Hulinga & K. Ozbay (2005). *Quantifying effects of ramp metering on freeway safety*. In the proceedings of annual meeting of Transportation Research Board, Washington DC, Jan. 9 – 13, Paper No. 05-0889.
5) K. Bilstrup, et al., (2009). *Report on collaboration between CVIS and CERES in the project vehicle alert system (VAS)* (Technical Report IDE09120), Halmsted University, Halmsted, Sweden.
6) J. M. Vianney Hakizimana (2007). *Investigation of services and application scenarios for inter-vehicle communication* (Technical report, IDE0751). Halmsted Univerisyt, Halmsted, Sweden.
7) X. Yang, J. Liu, Z. Zhao. (2004). *Vehicle-to-vehicle communication protocol for cooperative collision warning.* Retrieved from http://www.fengzhao.com/pubs/yang_x_v2v.pdf
8) S. Rezaei, R. Sengupta, & H. Krishnan. (2007). *Reducing the communication required by DSRC-based vehicle safety systems*. In proceedings of IEEE's Intelligent Transportation Systems Conference, pp. 361-366, Sept. 30–Oct. 3.
9) N. Kawanishi, R. Furukawa, S. Tang, A. Hasegawa, R. Miura, & Y. Takeuchi. (2013). *Simulation evaluation of cooperative relative positioning around intersections*. In proceedings of ITS Telecommunications (ITST), 2013 13th International Conference, pp. 372 – 377.
10) S. Tang, N. Kubo, & M. Ohashi. (2012). *Cooperative Relative Positioning for Intelligent Transportation System*. In Proc. 12th International Conference on ITS Telecommunications, pp. 506-511.
11) N. Alam, A. T. Balaei, & A. G. Dempster. (2013). Relative positioning enhancement in vanets: A tight integration approach. *IEEE Trans. Intell. Transp. Syst, 14*(1), 47–55 (cit. on pp. 2, 13).
12) J. Farrell & T. Givargis. (2000). Differential GPS reference station algorithm-design and analysis. *IEEE Transactions on Control Systems Technology, 8*(3), 519–531 (cit. on pp. 2, 9).
13) FHWA. (2003). High accuracy-nationwide differential global positioning system program fact sheet, FHWA-RD-03-039. Retrieved from http:// www. fhwa. dot. gov/publications/research/operations/03039/ (cit. on pp. 2, 9).
14) Z. Peng, S. Hussain, M. I. Hayee, & M. Donath. (2017). *Acquisition of relative trajectories of surrounding vehicles using GPS and DSRC based V2V communication with lane level resolution*. In proceedings of 3rd International Conference on Vehicle Technology and Intelligent Transport Systems, pp. 242–251.
15) A. S. Huang. (2010). Lane estimation for autonomous vehicles using vision and lidar. Retrieved from http://rvsn.csail.mit.edu/Pubs/phd_ ashuang_2010feb_laneestimation.pdf.

16) A. Selloum, D. Betaille, E. L. Carpentier, & F. Peyret. (2009). *Lane level positioning using particle filtering.* Paper presented at the 12th International IEEE Conference on Intelligent Transportation Systems, 2009, St. Louis, MO.
17) S. Lee, S.-W. Kim, & S.-W. Seo. (2015). *Accurate ego-lane recognition utilizing multiple road characteristics in a Bayesian network framework*. Paper presented at the IEEE Intelligent Vehicles Symposium (IV), 2015, Seoul, South Korea.
18) E. Casapietra, T. H. Weisswange, C. Goerick, F. Kummert, & J. Fritsch. (2015). *Building a probabilistic grid-based road representation from direct and indirect visual cues*. Paper presented at the 2015 IEEE Intelligent Vehicles Symposium (IV), 2015, Seoul, South Korea.
19) N. Alam, A. T. Balaei, & A. G. Dempster. (2013). Relative positioning enhancement in VANETs: A tight integration approach. *IEEE Trans. Intell. Transp. Syst., 14*(1), 47–55.
20) D. Chun, & K. Stol. (2012). *Vehicle motion estimation using low-cost optical flow and sensor fusion, Mechatronics and Machine Vision in Practice (M2VIP)*. In proceedings of the 19th International Conference on Mechatronics and Machine Vision in Practice (M2VIP), pp. 507–512, 2012, Auckland, New Zealand.
21) A. F. Abdelfatah, J. Georgy, U. Iqbal, A. Noureldin. (2011). 2*D Mobile multi-sensor navigation system realization using FPGA-based embedded processors.* In proceedings of the Canadian Conference on Electrical and Computer Engineering (CCECE), pp. 1218–1221. 2012, Niagra Falls, ON. Canada
22) Q. Li, L. Chen, M. Li, S.-L. Shaw, & A. Nuchter. (2014). A sensor-fusion drivable-region and lane-detection system for autonomous vehicle navigation in challenging road scenarios, vehicular technology. *IEEE Transactions, 63*(2), 540–555.
23) H. Zhao, M. Chiba, R. Shibasaki, X. Shao, J. Cui, & H. Zha. (2009) A laser-scanner-based approach toward driving safety and traffic data collection. *IEEE Trans. Intell. Transp. Syst., 10*(3), pp. 534-546.
24) A. Bansal, H. Badino, & D. Huber. (2014). Understanding how camera configuration and environmental conditions affect appearance-based localization. In Intelligent Vehicles Symposium Proceedings (IV), IEEE, 800–807.
25) G. Yu, Z. Wang, Y. Ma, & X. Wu. (2017). *Improved real-time lane detection using advanced lane extraction method*. Washington, DC: Transportation Research Board.
26) S. Sakjiraphong, A. Pinho, & M. N. Dailey. (2014). Real-time road lane detection with commodity hardware. Paper presented at the International Electrical Engineering Congress (iEECON), 2014, Chonburi, Thailand.
27) A. Assidiq, O. Khalifa, M. R. Islam, & S. Khan. (2008). *Real time lane detection for autonomous vehicles*. Paper presented at the 2008 International Conference on Computer and Communication Engineering, 2008, Kuala Lumpur, Malaysia.
28) R. Toledo-Moreo, M. A. Zamora-Izquierdo, B. Ubeda-Minarro, & A. F. Gomez-Skarmeta. (2007). High-integrity IMM-EKF-based road vehicle navigation with low-cost GPS/SBAS/INS. IEEE Trans. Intell. Transp.Syst., 8(3), 491–511.
29) N. Mattern, R. Schubert, & G. Wanielik. (2010*). High-accurate vehicle localization using digital maps and coherency images*. In Procedings of IEEE Intell. Vehicles Symp., pp. 462–469, La Jolla, CA.

30) R. G. García-García, M. A. Sotelo, I. Parra, D. Fernández, & M. Gavilán. (2007). *3D visual odometry for GPS navigation assistance*. In proceedings of IEEE Intell. Vehicles Symp., pp. 444–449.
31) J. Juang, & C. Lin. (2007). A sensor fusion scheme for the estimation of vehicular speed and heading angle, vehicular technology. *IEEE Transactions*, 64(7), 2773– 2782.
32) S. Rezaei & R. Sengupta. (2007). Kalman filter-based integration of DGPS and vehicle sensors for localization. *IEEE Trans. Control Syst. Technol., 15*(6), 1080–1088.
33) A. Vu, A. Ramanandan, A. Chen, J. A. Farrell, & M. Barth. (2012). Real-time computer vision/DGPS-aided inertial navigation system for lane-level vehicle navigation. *IEEE Transactions on Intelligent Transportation Systems, 13*(2), 899–913.
34) J. Du, & M. Barth. (2004). *Lane-level positioning for in-vehicle navigation and automated vehicle location (AVL) systems*. In proceedings of Int. IEEE 7th ITSC.
35) C. Guo, J. Meguro, K. Yamaguchi, K. Kidono, & Y. Kojima. (2014). *Improved lane detection based on past vehicle trajectories*. Paper presented at the 17th International IEEE Conference, pp. 1956-1963, 2014, Qingdao, China.
36) W. J. Hughes. (2014). *Global positioning system (GPS) standard positioning service (SPS) performance analysis report.* Washington, DC. Federal Aviation Administration.
37) D. K. Schrader. (2013). *Inexpensive GPS receivers to improve accuracy and reliability*. In proceedings of Sensors Applications Symposium (SAS), pp. 33–37 (cit. on p. 8), 2012. Brescia, Italy.
38) R. B. Langley. (1997). GPS receiver system noise. *GPS World, 8*(6), 40–45 (cit. on p. 8). Retrieved from http://gauss.gge.unb.ca/papers.pdf/gpsworld.june97.pdf
39) A. El-Rabbany. (2009). Introduction to GPS: The global positioning system. Published by Artech House Incorporated, 2nd edition, p. 29 (cit. on p. 9).
40) T. Kos, I. Markezic, & J. Pokrajcic. (2010). *Effects of multipath reception on GPS positioning performance*. In proceedings of ELMAR, 52nd International Symposium, pp. 399–402 (cit. on p. 11).
41) University of Wisconsin Greenbay. (2006). Converting UTM to latitude and longitude (or vice versa). Retrieved from https://www.uwgb.edu/dutchs/UsefulData/UTMFormulas.HTM
42) M. L. Timmons. (2013). Department of Transportation State Aid for Local Transportation Division, chapter 8820. Retrieved from http://www.dot.state.mn.us/stateaid/programlibrary/stateaidrules.pdf
43) A. S. Mihaita, P. Tyler, & A. Menon. (2017). An investigation of position accuracy transmitted by connected heavy vehicles using DSRC. Washington, DC: Transportation Research Board.